disruption of the thin fibrous cap may possibly cause embolization of the lipid components of the attenuated plaque to the distal coronary circulation causing transient or permanent coronary flow disturbance [17].

Lipid-rich attenuated plaque may be stabilized during follow-up. Xu et al. [8] reported that attenuation score defined based on the angle of the attenuation decreased and calcium score increased significantly during 14-month follow-up. Previous IVUS studies similarly demonstrated that patients with non-culprit lesion plaque ruptures who were treated with statins had good clinical outcomes [21, 22]. Although overall prognosis of the attenuated plaque was similar to that in non-attenuated plaque, it is known that slow flow/no reflow was associated with increased risk of cardiovascular events [23]. Therefore, slow flow/no reflow should be prevented if possible during PCI. Previous randomized studies suggested that routine use of distal protection device in patient with AMI did not improve clinical outcome after stenting [24, 25]. Alternatively, selective use of the distal protection device may be warranted based on the risk stratification using IVUS imaging [1, 4, 26]. A prospective, randomized trial to test the efficacy of the distal protection using Filtrap in patients at high risk (attenuated plaque $\geq$5 mm) for distal embolization during PCI in patients with ACS (VAMPIRE3 study, NCT01460966) is now underway. Results of the VAMPIRE3 will possibly clarify the role of distal protection in lesions with attenuated plaque.

Our present study has several limitations. First, this is a single-center small-sized retrospective analysis of the previously reported study population. Second, overall incidence of the cardiovascular events was low. In fact, incidence of cardiac death and congestive heart failure requiring hospitalization were numerically (but not significantly) higher in patients with attenuated plaque. Therefore, the results need to be confirmed by a prospective, multicenter large-scale study with properly sized population of patients. Third, radiofrequency signal-derived tissue characterization analysis [26–29] was not performed in this study because it was not available at the time of this study. Therefore, additional role of the tissue characterization to predict long-term clinical outcome is uncertain. Finally, prevalence of attenuated plaque in this study (66 %) was similar to a previous study (70 %) [8] but higher than another previous study (34 %) [4]. This may in part be explained by the difference in the study population and could have bias the results.

In conclusion, coronary plaque with ultrasonic attenuation or "attenuated plaque" was not related to long-term clinical outcome when coronary reflow after PCI was preserved.

Conflict of interest The authors declare that they have no conflict of interest.

References

1. Okura H, Taguchi H, Kubo T, Toda I, Yoshida K, Yoshiyama M, Yoshikawa J (2007) Atherosclerotic plaque with ultrasonic attenuation affects coronary reflow and infarct size in patients with acute coronary syndrome: an intravascular ultrasound study. Circ J 71:648–653
2. Lee SY, Mintz GS, Kim SY, Hong YJ, Kim SW, Okabe T, Pichard AD, Satler LF, Kent KM, Suddath WO, Waksman R, Weissman NJ (2009) Attenuated plaque detected by intravascular ultrasound: clinical, angiographic, and morphologic features and post-percutaneous coronary intervention complications in patients with acute coronary syndromes. JACC Cardiovasc Interv 2:65–72
3. Kimura S, Kakuta T, Yonetsu T, Suzuki A, Iesaka Y, Fujiwara H, Isobe M (2009) Clinical significance of echo signal attenuation on intravascular ultrasound in patients with coronary artery disease. Circ Cardiovasc Interv 2:444–454
4. Endo M, Hibi K, Shimizu T, Komura N, Kusama I, Otsuka F, Mitsuhashi T, Iwahashi N, Okuda J, Tsukahara K, Kosuge M, Ebina T, Umemura S, Kimura K (2010) Impact of ultrasound attenuation and plaque rupture as detected by intravascular ultrasound on the incidence of no-reflow phenomenon after percutaneous coronary intervention in ST-segment elevation myocardial infarction. JACC Cardiovasc Interv 3:540–549
5. Wu X, Mintz GS, Xu K, Lansky AJ, Witzenbichler B, Guagliumi G, Brodie B, Kellett MA Jr, Dressler O, Parise H, Mehran R, Stone GW, Maehara A (2011) The relationship between attenuated plaque identified by intravascular ultrasound and no-reflow after stenting in acute myocardial infarction: the HORIZONS-AMI (harmonizing outcomes with revascularization and stents in acute myocardial infarction) trial. JACC Cardiovasc Interv 4:495–502
6. Wu X, Maehara A, Mintz GS, Kubo T, Xu K, Choi SY, He Y, Guo N, Moses JW, Leon MB, De Bruyne B, Serruys PW, Stone GW (2010) Virtual histology intravascular ultrasound analysis of non-culprit attenuated plaques detected by grayscale intravascular ultrasound in patients with acute coronary syndromes. Am J Cardiol 105:48–53
7. Yamada R, Okura H, Kume T, Neishi Y, Kawamoto T, Watanabe N, Toyota E, Yoshida K (2007) Histological characteristics of plaque with ultrasonic attenuation: a comparison between intravascular ultrasound and histology. J Cardiol 50:223–228
8. Xu K, Mintz GS, Kubo T, Wu X, Guo N, Yang J, Witzenbichler B, Guagliumi G, Brodie B, Dressler O, Cristea E, Parise H, Mehran R, Stone GW, Maehara A (2012) Long-term follow-up of attenuated plaques in patients with acute myocardial infarction: an intravascular ultrasound substudy of the HORIZONS-AMI trial. Circ Cardiovasc Interv 5:185–192
9. Sakata Y, Kodama K, Ishikura F, Komamura K, Hasegawa S, Hirayama A (1997) Disappearance of the 'no-reflow' phenomenon after adjunctive intracoronary administration of nicorandil in a patient with acute myocardial infarction. Jpn Circ J 61:455–458
10. Tsubokawa A, Ueda K, Sakamoto H, Iwase T, Tamaki S (2002) Effect of intracoronary nicorandil administration on preventing no-reflow/slow flow phenomenon during rotational atherectomy. Circ J 66:1119–1123
11. Iwasaki K, Samukawa M, Furukawa H (2006) Comparison of the effects of nicorandil versus verapamil on the incidence of slow flow/no reflow during rotational atherectomy. Am J Cardiol 98:1354–1356
12. Matsuo H, Watanabe S, Watanabe T, Warita S, Kojima T, Hirose T, Iwama M, Ono K, Takahashi H, Segawa T, Minatoguchi S, Fujiwara H (2007) Prevention of no-reflow/slow-flow phenomenon during rotational atherectomy—a prospective randomized

study comparing intracoronary continuous infusion of verapamil and nicorandil. Am Heart J 154(994):e1–e6
13. Wang HJ, Lo PH, Lin JJ, Lee H, Hung JS (2004) Treatment of slow/no-reflow phenomenon with intracoronary nitroprusside injection in primary coronary intervention for acute myocardial infarction. Catheter Cardiovasc Interv 63:171–176
14. Kobatake R, Sato T, Fujiwara Y, Sunami H, Yoshioka R, Ikeda T, Saito H, Ujihira T (2011) Comparison of the effects of nitroprusside versus nicorandil on the slow/no-reflow phenomenon during coronary interventions for acute myocardial infarction. Heart Vessels 26:379–384
15. Burzotta F, Trani C, Romagnoli E, Mazzari MA, Rebuzzi AG, De Vita M, Garramone B, Giannico F, Niccoli G, Biondi-Zoccai GG, Schiavoni G, Mongiardo R, Crea F (2005) Manual thrombus-aspiration improves myocardial reperfusion: the randomized evaluation of the effect of mechanical reduction of distal embolization by thrombus-aspiration in primary and rescue angioplasty (REMEDIA) trial. J Am Coll Cardiol 46:371–376
16. Ikari Y, Sakurada M, Kozuma K, Kawano S, Katsuki T, Kimura K, Suzuki T, Yamashita T, Takizawa A, Misumi K, Hashimoto H, Isshiki T (2008) Upfront thrombus aspiration in primary coronary intervention for patients with ST-segment elevation acute myocardial infarction: report of the VAMPIRE (VAcuuM asPIration thrombus REmoval) trial. JACC Cardiovasc Interv 1:424–431
17. Kotani J, Nanto S, Mintz GS, Kitakaze M, Ohara T, Morozumi T, Nagata S, Hori M (2002) Plaque gruel of atheromatous coronary lesion may contribute to the no-reflow phenomenon in patients with acute coronary syndrome. Circulation 106:1672–1677
18. Iwakura K, Ito H, Kawano S, Okamura A, Kurotobi T, Date M, Inoue K, Fujii K (2006) Chronic pre-treatment of statins is associated with the reduction of the no-reflow phenomenon in the patients with reperfused acute myocardial infarction. Eur Heart J 27:534–539
19. Kubo T, Matsuo Y, Ino Y, Tanimoto T, Ishibashi K, Komukai K, Kitabata H, Tanaka A, Kimura K, Imanishi T, Akasaka T (2011) Optical coherence tomography analysis of attenuated plaques detected by intravascular ultrasound in patients with acute coronary syndromes. Cardiol Res Pract 2011:687515
20. Lee T, Kakuta T, Yonetsu T, Takahashi K, Yamamoto G, Iesaka Y, Fujiwara H, Isobe M (2011) Assessment of echo-attenuated plaque by optical coherence tomography and its impact on post-procedural creatine kinase-myocardial band elevation in elective stent implantation. JACC Cardiovasc Interv 4:483–491
21. Rioufol G, Gilard M, Finet G, Ginon I, Boschat J, Andre-Fouet X (2004) Evolution of spontaneous atherosclerotic plaque rupture with medical therapy: long-term follow-up with intravascular ultrasound. Circulation 110:2875–2880
22. Hong MK, Mintz GS, Lee CW, Suh IW, Hwang ES, Jeong YH, Park DW, Kim YH, Han KH, Cheong SS, Kim JJ, Park SW, Park SJ (2007) Serial intravascular ultrasound evidence of both plaque stabilization and lesion progression in patients with ruptured coronary plaques: effects of statin therapy on ruptured coronary plaque. Atherosclerosis 191:107–114
23. Ito H (2006) No-reflow phenomenon and prognosis in patients with acute myocardial infarction. Nat Clin Pract Cardiovasc Med 3:499–506
24. Stone GW, Webb J, Cox DA, Brodie BR, Qureshi M, Kalynych A, Turco M, Schultheiss HP, Dulas D, Rutherford BD, Antoniucci D, Krucoff MW, Gibbons RJ, Jones D, Lansky AJ, Mehran R (2005) Distal microcirculatory protection during percutaneous coronary intervention in acute ST-segment elevation myocardial infarction: a randomized controlled trial. JAMA 293:1063–1072
25. Muramatsu T, Kozuma K, Tsukahara R, Ito Y, Fujita N, Suwa S, Koyama S, Saitoh M, Kamiya H, Nakamura M (2007) Comparison of myocardial perfusion by distal protection before and after primary stenting for acute myocardial infarction: angiographic and clinical results of a randomized controlled trial. Catheter Cardiovasc Interv 70:677–682
26. Kawamoto T, Okura H, Koyama Y, Toda I, Taguchi H, Tamita K, Yamamuro A, Yoshimura Y, Neishi Y, Toyota E, Yoshida K (2007) The relationship between coronary plaque characteristics and small embolic particles during coronary stent implantation. J Am Coll Cardiol 50:1635–1640
27. Yamada R, Okura H, Kume T, Neishi Y, Kawamoto T, Miyamoto Y, Imai K, Saito K, Tsuchiya T, Hayashida A, Yoshida K (2010) Target lesion thin-cap fibroatheroma defined by virtual histology intravascular ultrasound affects microvascular injury during percutaneous coronary intervention in patients with angina pectoris. Circ J 74:1658–1662
28. Miyamoto Y, Okura H, Kume T, Kawamoto T, Neishi Y, Hayashida A, Yamada R, Imai K, Saito K, Yoshida K (2011) Plaque characteristics of thin-cap fibroatheroma evaluated by OCT and IVUS. JACC Cardiovasc Imaging 4:638–646
29. Takaoka N, Tsujita K, Kaikita K, Hokimoto S, Yamanaga K, Komura N, Chitose T, Ono T, Mizobe M, Horio E, Sato K, Nakayama N, Saito M, Iwashita S, Kojima S, Tayama S, Sugiyama S, Nakamura S, Ogawa H (2013) Intravascular ultrasound morphology of culprit lesions and clinical demographics in patients with acute coronary syndrome in relation to low-density lipoprotein cholesterol levels at onset. Heart Vessels. doi:10.1007/s00380-013-0401-7

International Journal of Cardiology 178 (2015) 239–246

Contents lists available at ScienceDirect

International Journal of Cardiology

journal homepage: www.elsevier.com/locate/ijcard

Repeated remote ischemic conditioning attenuates left ventricular remodeling via exosome-mediated intercellular communication on chronic heart failure after myocardial infarction

Takehiro Yamaguchi [a], Yasukatsu Izumi [b,*], Yasuhiro Nakamura [a,c], Takanori Yamazaki [a], Masayuki Shiota [b], Soichi Sano [a], Masako Tanaka [b,d], Mayuko Osada-Oka [e], Kenei Shimada [a], Katuyuki Miura [b,d], Minoru Yoshiyama [a], Hiroshi Iwao [b,f]

[a] Department of Cardiovascular Medicine, Osaka City University Medical School, Osaka, Japan
[b] Department of Pharmacology, Osaka City University Medical School, Osaka, Japan
[c] Department of Cardiology, Izumi Municipal Hospital, Izumi, Japan
[d] Applied Pharmacology and Therapeutics, Osaka City University Medical School, Osaka, Japan
[e] Food Hygiene and Environmental Health Division of Applied Life Science, Kyoto Prefectural University, Kyoto, Japan
[f] Department of Education, Shitennoji University, Habikino, Japan

ARTICLE INFO

Article history:
Received 13 August 2014
Received in revised form 24 September 2014
Accepted 22 October 2014
Available online 30 October 2014

Keywords:
Exosomes
Left ventricular dysfunction
MicroRNA
Myocardial infarction
Remote ischemic conditioning

ABSTRACT

Background: Remote ischemic conditioning (RIC) by repeated treatment of transient limb ischemia is a clinically applicable method for protecting the heart against injury at the time of reperfusion. In this study, we investigated the effects of repeated RIC on cardiac dysfunction after myocardial infarction (MI).
Methods and results: At 4 weeks after MI, rats were separated into the untreated (UT) group or the RIC-treated group. RIC treatment was performed by 5 cycles of 5 min of bilateral hindlimb ischemia and 5 min of reperfusion once a day for 4 weeks. Despite comparable MI size, left ventricular (LV) ejection fraction (LVEF) was significantly improved in the RIC group compared with the UT group. Furthermore, the LVEF in the RIC group was improved, although not significantly, after treatment. RIC treatment also prevented the deterioration of LV diastolic function. MI-induced LV interstitial fibrosis in the boundary region and oxidant stress were significantly attenuated by RIC treatment. MicroRNA-29a (miR-29a), a key regulator of tissue fibrosis, was highly expressed in the exosomes and the marginal area of the RIC group. Even in the differentiated C2C12-derived exosomes, miR-29a expression was significantly increased under hypoxic condition. As well as miR-29a, insulin-like growth factor 1 receptor (IGF-1R) was highly expressed both in the exosomes and remote non-infarcted myocardium of the RIC group. IGF-1R expression was also increased in the C2C12-derived exosomes under hypoxic conditions.
Conclusions: Repeated RIC reduces adverse LV remodeling and oxidative stress by MI. Exosome-mediated intercellular communication may contribute to the beneficial effect of RIC treatment.

1. Introduction

Chronic heart failure (CHF) is a clinical syndrome representing the end-stage of a number of different cardiac diseases. It causes exercise intolerance, impairs quality of life, and has been associated with high morbidity and mortality. Although the existing pharmacological therapies, such as inhibitors of the renin–angiotensin–aldosterone system and β-adrenoreceptor blockers improved outcomes in CHF [1–4], they are still not optimal and cannot fully prevent progressive cardiac remodeling and dysfunction. Recently, several non-pharmacological therapies such as cardiac rehabilitation and ventilatory support have been developed [5,6]. However, these therapies are associated with tolerability issues, and not all CHF patients benefit from them. Therefore, there is a need to develop a novel therapy that is easy to perform and is well tolerated.

The cardioprotective effect of remote ischemic preconditioning was originally reported by Przykelenk et al. [7]. They reported that ischemic preconditioning in the left circumflex coronary artery attenuated ischemia-reperfusion (IR) injury by subsequent occlusion of the left anterior descending coronary artery (LAD). Thereafter, some reports have shown that ischemic preconditioning [8,9] and postconditioning [10,11] of the extremities can protect the heart from IR injury. Thus, remote ischemic conditioning (RIC) may be one of the therapeutic strategies for protecting organs or tissue against IR injury. Briefly repeated non-lethal ischemia and reperfusion of a remote organ or tissue increase heart tolerability to acute IR injury. Although various studies supported

* Corresponding author at: Department of Pharmacology, Osaka City University Medical School, 1-4-3 Asahimachi, Abeno-ku, Osaka 545-8585, Japan.
E-mail address: izumi@msic.med.osaka-cu.ac.jp (Y. Izumi).

http://dx.doi.org/10.1016/j.ijcard.2014.10.144
0167-5273/

the beneficial effect of RIC against acute myocardial infarction (MI), it is still unclear whether RIC is beneficial for CHF.

In this study, we hypothesized that the efficacy of RIC can expand not only to IR injury in the acute phase of MI but to left ventricular (LV) dysfunction in the chronic phase of MI. Our results showed that RIC treatment improved LV dysfunction and attenuated LV interstitial fibrosis in an experimental CHF model. These results may have clinical implications for the treatment of patients with evolving LV dysfunction.

2. Methods

2.1. Animals and experimental design

All procedures were performed in accordance to Osaka City University animal care guidelines, which conform to the Guide for the Care and Use of Laboratory Animals published by the US National Institutes of Health (NIH Publication No. 85-23, revised 1996). The 8-week-old male Wistar rats weighing 260–290 g were purchased from CLEA Japan, Inc (Osaka, Japan).

The rats were intubated and were under mechanical ventilation with adequate anesthesia by pentobarbital (50 $mg \cdot kg^{-1}$, intraperitoneally). Then, MI was induced by permanent ligation of the left coronary artery, as described previously [12,13]. Excluding the suturing of the coronary artery, the same surgical procedure was performed on a control group of rats.

At 4 weeks after MI induction, blood pressure (BP) and heart rate (HR) of the rats by the tail cuff method (BP98A; Softron, Tokyo, Japan) were measured and transthoracic echocardiography was performed to assess cardiac function. Basing on the echocardiographic findings, MI-induced rats were divided into two groups: the RIC-treated (RIC) group and untreated (UT) group (Fig. 1A). The sham-operated rats were used as the control group.

After 4 weeks of treatment, the BP and HR of the rats were measured. Under anesthesia, cardiac function was assessed by echocardiography. Immediately after echocardiography, the rat abdomen was cut open, and a blood sample was collected from the inferior vena cava. The hearts were then immediately excised, and the ventricle was separated from the atrium and was weighed.

The infarct size was calculated as the ratio of the scar area to the entire cardiac muscle area. The ventricle was separated into the upper and lower portions, and then the upper portion of the left ventricle was divided into the marginal zone and non-infarcted zone; the specimens obtained were then immediately frozen in liquid nitrogen and stored at −80 °C until use. The lower portion was fixed in 10% formaldehyde overnight and embedded in paraffin.

2.2. RIC treatment

The rats in all groups were adequately anesthetized with pentobarbital, and the bilateral hindlimbs of rats in the RIC group were subjected to repeated transient ischemia: 5 cycles of 5 min of bilateral hindlimb ischemia and 5 min of reperfusion, by tourniquets [11]. RIC treatment was performed once a day for 4 weeks (Fig. 1B).

2.3. Echocardiographic study

Transthoracic echocardiography was performed using a Xario ultrasound device (Toshiba Medical Systems, Tokyo, Japan) with a 6-MHz cardiac transducer, according to previously described methods [12,13]. In brief, rats were anesthetized with pentobarbital. A two-dimensional short-axis view of the left ventricle was obtained at the level of the papillary muscles. The LV ejection fraction (LVEF) was calculated by measuring the LV end-diastolic volume (LVEDV) and the LV end-systolic volume (LVESV), by using a modified Simpson's method. Pulsed wave Doppler spectra (early rapid filling [E] wave and atrial contraction [A] wave) of mitral inflow velocities were recorded from the apical 4-chamber view, with the sample volume placed near the tips of the mitral leaflets and adjusted to the position at which velocity was maximum and the flow pattern was laminar, and the ratio of E wave velocity to A wave velocity (E/A) was calculated. The early velocity of the mitral annulus (e′) was determined by tissue Doppler imaging. The ratio of the E wave velocity to e′ wave velocity (E/e′) was calculated.

2.4. Histological assessment and evaluation of oxidative stress

The area of interstitial fibrosis in the marginal area of the infarct was measured, as described previously [13–15]. In brief, 4-μm-thick sections were cut and stained with hematoxylin–eosin stain and Sirius red stain. The fibrosis area was calculated as the ratio of the sum of the total area of interstitial fibrosis to the sum of the total connective tissue area plus the area of cardiomyocytes in the marginal area of the LV. Each field was analyzed using image-analyzing software (Micro Analyzer, Japan Poladigital, Tokyo, Japan).

The serum levels of derivatives of reactive-oxygen metabolites (d-ROMs) were measured by the Free Radical Elective Evaluator (Diacron International, Grosseto, Italy) using commercial assay kits (Diacron International).

2.5. Exosome purification

Exosomes were purified from serum or culture media by the ultracentrifugation method, as previously reported [16]. In brief, each serum sample was centrifuged for eliminating debris and cellular components at 2000 ×g for 30 min at 4 °C, and then at 10,000 ×g for 30 min at 4 °C. Next, supernatants were ultracentrifuged at 10,000 ×g for 3 h at 4 °C. After washing with phosphate buffered saline (PBS), exosome pellets were dissolved in PBS and stored at −80 °C until use. The amount of exosome protein was quantified by BCA assay (ThermoScientific, Waltham, MA, USA).

2.6. RNA and MicroRNA expression analysis

Total RNA and microRNA were extracted from tissues or exosomes with Isogen II (Nippon Gene, Toyama, Japan). The concentration and quality of RNA were assessed by the Nano Drop 2000 (Thermo, Waltham, MA, USA). To quantify the gene expression levels,

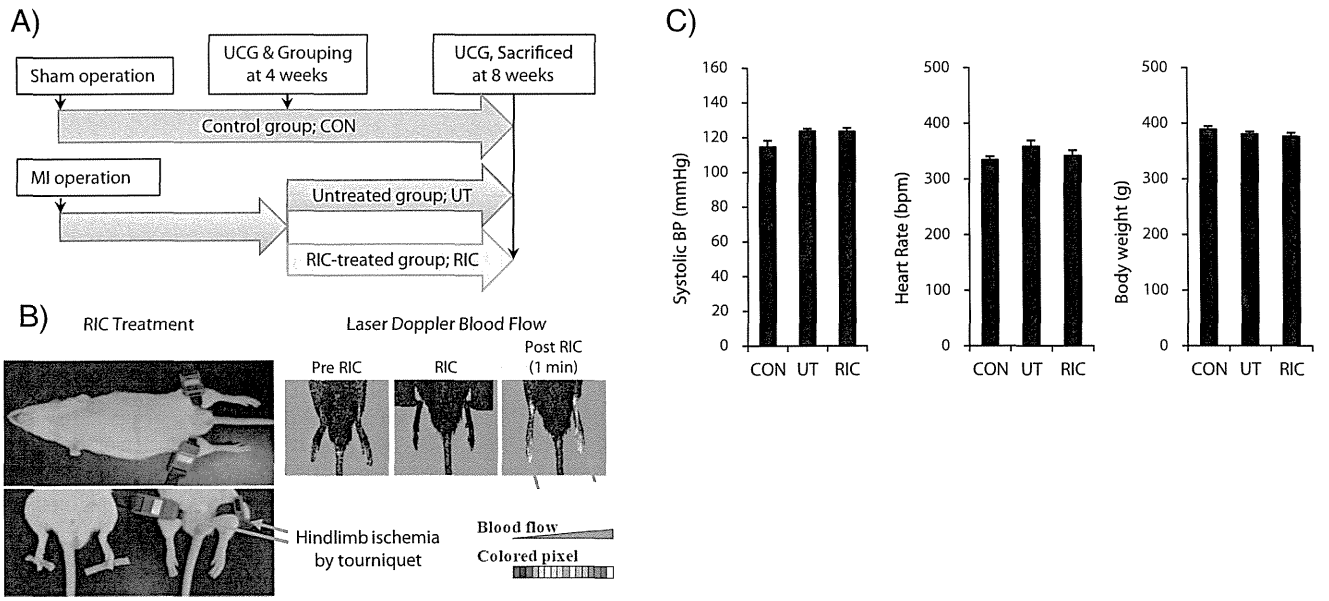

Fig. 1. Experimental protocols and hemodynamics. (A) The protocol of the present study is shown. At 4 weeks after the induction of MI, the rats were divided into the untreated group and RIC-treated group. (B) Transient ischemia was produced in the bilateral hindlimbs of the rats by tourniquets (left panel). A decrease in blood flow during RIC treatment was confirmed by a laser Doppler. Blood flow in the hindlimbs was more increased after the tourniquets were released (right panel, arrow). (C) Hemodynamic status and body weight of each group. All values are mean ± SEM (n = 11 to 17). UCG, ultrasound cardiography; MI, myocardial infarction; CON, control group; UT, untreated group; RIC, remote ischemic conditioning group; BP, blood pressure.

we performed quantitative real-time reverse transcription polymerase chain reaction (RT-PCR) by the TaqMan system (Applied Biosystems, CA, USA), as previously described [13]. For normalization the transcript levels were compared to those of GAPDH.

Reverse transcription of microRNA was performed with a miScript II RT Kit (Qiagen, Hilden, Germany). For quantitative real-time PCR of microRNA, miScript SYBR Green PCR Kit and miScript Primer Assay specific for miR-21, miR-29a, miR-30a, and miR-133a were used. For normalization, the transcript levels were compared to those of RNU-6.

2.7. Cells

C2C12 cells, which were kindly gifted by Mr. Ohkawa (Kyushu University), were maintained in high-glucose Dulbecco's modified Eagle's medium (DMEM) (Wako Pure Chemical Industries, Osaka, Japan) supplemented with 20% fetal bovine serum. Near-confluent cells were induced to differentiate by DMEM with 2% horse serum [17]. Differentiated C2C12 cells were incubated under normoxic condition (21% O_2 and 5% CO_2 at 37 °C) and hypoxic condition (1% O_2 and 5% CO_2 at 37 °C) for 24 h. Eoxsomes were purified from culture media in the same way as serum.

2.8. Western blot analysis

Proteins from the rat heart and the serum exosomes were extracted in RIPA buffer (20 mM Tris–HCl, pH 7.4, 150 mM sodium chloride, 2 mM EGTA, 0.5% sodium deoxycholate, 1% Triton-X 100, 100 mM sodium fluoride, and 2 mM sodium orthovanadate) containing protease inhibitors (Protease inhibitors Cocktail, Nacalai, Kyoto, Japan), and the concentration of protein extracted from each specimen was quantified by the BCA protein assay kit. Separated proteins by SDS-PAGE were transferred to Immobilon-P PVDF membranes (Millipore, MA, USA). The membranes were probed with the antibody of insulin-like growth factor-1 (IGF-1) receptor (IGF-1R) and heat shock protein (Hsp) 90 from Cell Signaling Technology (Beverly, MA, USA), CD9 from GeneTex (Irvine, CA, USA), collagen type III from SouthernBiotech (Birmingham, AL, USA), or HIF-1α from Cayman Chemical Company (Ann Arbor, MI). As a loading control, the membranes were stained using the PROTOGOLD kit (BBI Solutions, Cardiff, UK).

2.9. Statistical analysis

All data are presented as means ± SEM. For differences between two groups, a Student's *t* test was used when appropriate. Comparisons among groups were made using one-way analysis of variance followed by Fisher's protected least significant difference test by using StatView (SAS Institute, Inc., Cary, NC, USA). The differences between the values before and after treatment were analyzed by using Wilcoxon signed-rank tests. The differences were considered statistically significant at a value of $P < 0.05$.

3. Results

3.1. Effects of RIC treatment on hemodynamic status and body weight

Laser Doppler blood flow measurement was performed to confirm successful transient hindlimb ischemia by RIC treatment (Fig. 1B). During RIC treatment, blood flow in the hindlimb was diminished. Since the tourniquet was released, blood flow was recovered; moreover increased. Despite the increase of peripheral blood flow after RIC treatment, there was no significant difference in hemodynamic status such as BP and HR among the groups (Fig. 1C). Thus, RIC does not affect hemodynamic status. Furthermore, there was no significant difference in body weight among the groups (Fig. 1C).

3.2. RIC treatment rescues deterioration of LV dysfunction

Regarding echocardiographic evaluation, end-systolic and end-diastolic dimensions, and systolic function at 4 weeks after MI induction were similar between the UT and the RIC group. However, LV end-systolic dimension, LVEDV, and LDESV were significantly decreased and LVEF was significantly improved in the RIC group compared with the UT group at 8 weeks after MI induction (4 weeks after treatment) (Fig. 2A–D and Table 1). Four weeks of RIC treatment tended to improve LVEF, while lack of treatment worsened it (Table 1). There was no difference in the diastolic function including E/A between the UT and the RIC groups. Though there was no difference in E wave, A wave and E/A ratio between the UT and RIC groups, RIC treatment prevented the deterioration of e′ wave and significantly decreased E/e′ (Fig. 2E and Table 1).

3.3. RIC treatment suppresses LV remodeling

Light micrographs of a cross section of the midportion of the left ventricle (Fig. 3A) revealed that the LV size in the RIC group tended to be smaller than that in the UT group. The coefficient of ventricular weight to body weight (VW/BW), which was increased by MI induction, was significantly decreased in the RIC group compared with the UT group (2.72 ± 0.07 vs 2.51 ± 0.03 mg/g, respectively). RIC treatment significantly attenuated MI-induced LV interstitial fibrosis in the marginal area (25.0 ± 0.8% vs 15.8 ± 0.7%, respectively, Fig. 3C and D).

It is well known that oxidative stress involves remodeling of organs or tissue [18]. MI-induced elevation of the oxidative stress may deteriorate fibrosis and remodeling of the left ventricle. However, RIC treatment reduced the elevation of the oxidative stress (Fig. 3E) (UT; 605 ± 27 vs RIC; 495 ± 23 U.CARR).

3.4. Gene expressions and protein levels in the marginal area of the infarction

The expressions of fibrosis-related genes such as transforming growth factor-β (TGF-β), collagen type I (COL1A), and collagen type III (COL3A) were analyzed. There was no significant difference in these expressions between the UT and RIC groups (Fig. 4A). On the other hand, the protein level of COL3A was significantly suppressed in the RIC group than that in the UT group (Fig. 4B and C). Gene expressions of atrial natriuretic peptide (ANP) and brain natriuretic peptide (BNP) in the marginal area were similar between the UT and RIC groups.

3.5. The expressions of fibrosis-related microRNAs in the exosomes and marginal area of the infarction

Fibrosis-related microRNA expressions such as miR-21, miR-29a, miR-30a, and miR-133a [19] in the exosomes were analyzed. As shown in Fig. 5A, the expression of miR-29a, which negatively regulates tissue fibrosis [20], was significantly increased in the RIC group compared with the UT group. The expression of miR-30a known as a negative regulator of tissue fibrosis [21], tended to be higher in the RIC group than that in the UT group. In contrast, there was no significant difference in the miR-21 expression among the groups, which positively contributes to tissue fibrosis [22].

We also analyzed microRNA expressions in the marginal area of the infarction (Fig. 5B). Interestingly, the expressions of miR-29a and miR-30a were significantly higher in the RIC group than the UT group, just like their expressions in serum exosomes. Furthermore, hypoxia significantly increased miR-29a expression in exosomes from the media of C2C12 cells (Fig. 5C).

3.6. High expression of IGF-1R in the exosomes by RIC treatment

RIC treatment significantly increased the amount of protein in exosomes (Fig. 6A). Western blot analysis showed that CD9 and Hsp90, which are markers of exosomes, were detected in the exosomes purified from serum (Fig. 6B). IGF-1R was highly expressed only in the serum-derived exosomes of the RIC group. IGF-1R was also highly expressed in the remote non-infarcted myocardium of the RIC group (Fig. 6C and D). Furthermore, IGF-1R was increased in skeletal muscles of the hindlimbs of the RIC group (Fig. 6E and F). In vitro study also showed that hypoxia increased IGF-1R level not in cell lysates but in exosomes from culture media (Fig. 6G). These data suggest that IGF-1R may be transferred from the hindlimbs into the cardiomyocytes via exosome-mediated intercellular communication.

4. Discussion

Ischemic conditioning is well known as a novel strategy of protecting IR injury in coronary heart diseases, and is attracting

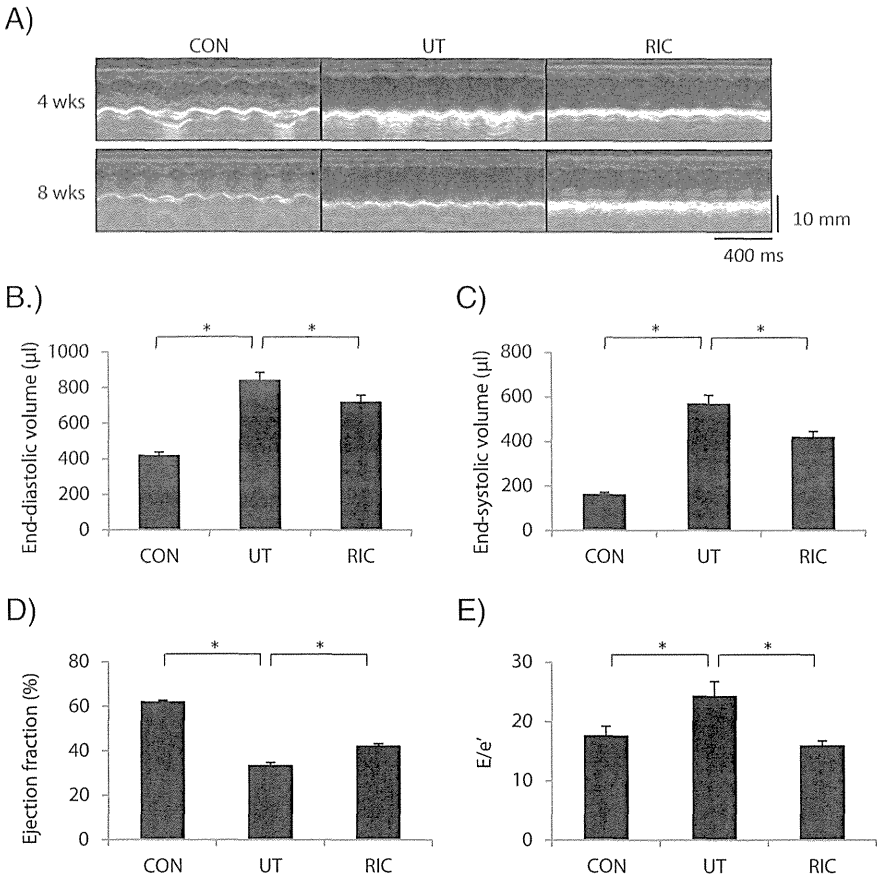

Fig. 2. Echocardiographic measurements at 4 weeks (before treatment) and 8 weeks (after treatment). (A) Representative M-mode echocardiography from each group. Graphs show the LVEDV (B), LVESV (C), LVEF (D), and E/e′ (E) after treatment. At 8 weeks after MI (after treatment), LVEDV and LVESV were significantly lower in the RIC group than those in the UT group. RIC-treated groups had significantly greater improvement in LVEF than the UT group. E/e′ was also improved by RIC treatment. All values are mean ± SEM (n = 11 to 17). *$P < 0.05$. LVEDV, left ventricular end-diastolic volume; LVESV, left ventricular end-systolic volume; LVEF, left ventricular ejection fraction; MI, myocardial infarction. Other abbreviations are the same as in Fig. 1 legend.

extensive interest of clinical cardiologists. Cardiomyocytes acquire tolerability against IR injury not only by ischemic conditioning of itself, but also by ischemic conditioning of remote organs. Recent studies indicate that RIC treatment reduces the infarct size due to MI [23]. We focused on the possibility of therapeutic effect of RIC against CHF and demonstrated the beneficial effect of repeated RIC treatment on the chronic phase of MI.

In the present study, RIC treatment prevented the deterioration of LV systolic and diastolic dysfunctions (Fig. 2). Of note, the increase of the heart weight and LV interstitial fibrosis due to MI induction was

Table 1
Echocardiographic findings.

	4 weeks after MI (baseline)			8 weeks after MI (baseline)		
	CON	UT	RIC	CON	UT	RIC
Dd (mm)	8.1 ± 0.1	10.2 ± 0.2*	10.1 ± 0.2	8.4 ± 0.2	10.5 ± 0.3*	9.9 ± 0.2
Ds (mm)	5.3 ± 0.1	8.4 ± 0.2*	8.2 ± 0.2	5.5 ± 0.2	8.7 ± 0.3*	7.9 ± 0.3**
FS (%)	34.5 ± 0.8	17.9 ± 1.3*	19.3 ± 1.4	33.9 ± 2.0	17.5 ± 1.2*	20.3 ± 1.5
EDV (μl)	391 ± 14	790 ± 71*	749 ± 29	420 ± 19	854 ± 70*	697 ± 53**
ESV (μl)	160 ± 11	484 ± 53*	462 ± 29	161 ± 10	577 ± 58*	413 ± 41**
EF (%)	61.9 ± 0.8	42.1 ± 1.5*	42.8 ± 1.9	61.9 ± 0.9	37.9 ± 2.0****	47.3 ± 2.4**
E (cm/s)	67.7 ± 2.1	78.7 ± 4.1	73.7 ± 2.9	68.9 ± 3.4	69.7 ± 4.2	67.6 ± 4.1
A (cm/s)	44.1 ± 2.3	47.6 ± 3.2	50.9 ± 2.6	45.6 ± 1.9	47.8 ± 3.7	52.3 ± 2.4
E/A	1.6 ± 0.1	1.8 ± 0.1	1.5 ± 0.1	1.5 ± 0.1	1.5 ± 0.1	1.3 ± 0.1
e′ (cm/s)	3.4 ± 0.1	3.9 ± 0.2	3.6 ± 0.3	3.9 ± 0.3	3.0 ± 0.2****	4.1 ± 0.2**
E/e′	19.6 ± 0.6	21.9 ± 2.2	21.2 ± 1.7	17.6 ± 1.6	24.3 ± 2.5*	15.9 ± 0.9*****

MI, myocardial infarction; CON, control group; UT, untreated group; RIC, remote ischemic conditioning group; LVDd, left ventricular end-diastolic diameter; LVDs, left ventricular end-systolic diameter; FS, fractional shortening; LVEDV, left ventricular end-diastolic volume; LVESV, left ventricular end-systolic volume, EF, ejection fraction; E/A, ratio of E wave velocity to A wave velocity; E/A, ratio of E wave velocity to e′ wave velocity. All data are presented as mean ± SEM.

* $P < 0.05$ (comparison between CON and UT at each week).

** $P < 0.05$ (comparison between UT and RIC at each week).

*** $P < 0.05$ (comparison between the parameters of 4 and 8 weeks in each group).

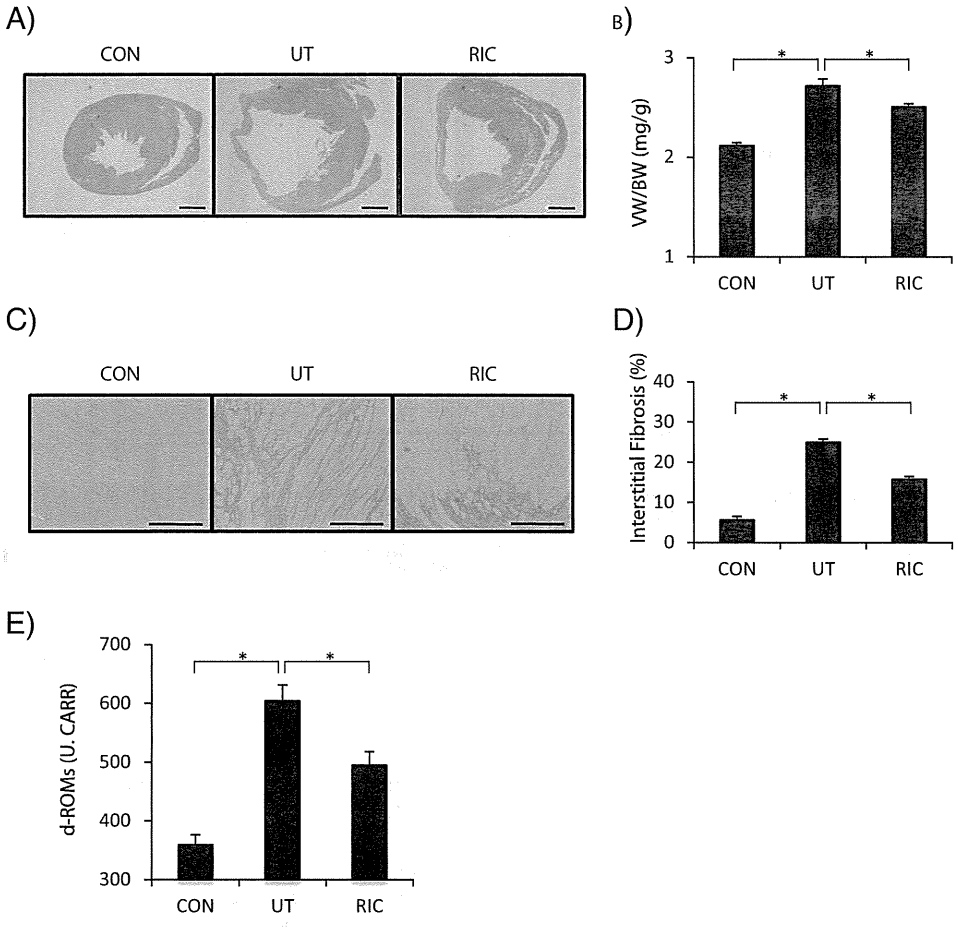

Fig. 3. Estimation of ventricular weight, the extent of interstitial fibrosis, and oxidant stress. (A) Representative photomicrographs of hematoxylin–eosin stained ventricular sections from each group (original magnification × 12.5). Bar, 2 mm. (B) The value of ventricular weight/body weight (VW/BW) in the untreated (UT) group was significantly higher than that in the control (CON) group. This increase was significantly suppressed in the remote ischemic conditioning (RIC) group. Values are mean ± SEM (n = 11 to 17). $^*P < 0.05$. (C) Representative photomicrographs of the cross-sections showing myocardial interstitial fibrosis by staining left ventricular marginal area sections (original magnification × 200) with Sirius red (red). Bar, 500 μm. (D) Quantitative results of relative area of interstitial fibrosis (%). The RIC group showed significantly greater suppression of MI-induced interstitial fibrosis than the UT group. Values are mean ± SEM (n = 11 to 17). $^*P < 0.05$. (E) Serum oxidative stress of each group was assessed by derivatives of reactive oxygen metabolites (d-ROMs). The RIC group exhibited a lower level of serum d-ROMs than the UT group. Values are mean ± SEM (n = 11 to 17). $^*P < 0.05$.

suppressed by RIC treatment (Fig. 3C and D), suggesting that RIC treatment may attenuate cardiac remodeling.

Oxidative stress is another important factor involved in cardiac remodeling [18]. The serum level of d-ROMs was higher in our MI-induced heart failure model rats than that in the sham-operated rats. Interestingly, RIC treatment significantly decreased the level (Fig. 3E), indicating that RIC treatment could decrease systemic oxidative stress via the compensatory actions of some antioxidative systems, though the precise mechanisms of these results are unclear.

To clear the mechanisms of RIC treatment, we focused on exosome-mediated intercellular communications. Exosome, which is an extracellular vesicle of 40–100 nm in diameter and contains proteins, mRNAs, microRNAs, and DNA [24,25], is considered to be a carrier of the information of intercellular communication [26]. Various cells release microRNAs in exosomes, which circulate stably in the bloodstream [27–30]. Although the physiological significance of circulating microRNAs is not fully elucidated, they were noted as potential diagnostic and prognostic biomarkers for various diseases [28–30]. Several microRNAs including miR-21 and miR-29 are known to be implicated in tissue fibrosis [19–22]. In particular, miR-29 family targets a cadre of mRNAs that encode proteins involved in fibrosis [20]. Our study demonstrated that MI induction decreased the expression of miR-29a (one of the miR-29 family) in the marginal area, and that RIC treatment restored the MI-induced down regulation of miR-29a. Interestingly, the expression of miR-29a in exosomes was increased in the RIC group. These findings suggest that exosomal miR-29a with RIC treatment may be endocytosed into the heart. The anti-fibrotic effect of miR-29a via exosome-mediated transmission may be a major mechanism of RIC treatment.

One of the candidate cells which release the exosomes by RIC treatment may be skeletal muscles because the treatment induces transient ischemia in the hindlimbs. In fact, hypoxia induced miR-29a expression in C2C12 cell-related exosomes (Fig. 5C). These data support that exosomes may be released in the hindlimbs and endocytosed into cardiomyocytes when the hindlimbs are subjected to RIC treatment. Consequently, RIC treatment may increase the tolerability of cardiomyocytes against developing remodeling.

IGF-1 signaling, which is considered to play a role in the prevention of progressive cardiac remodeling, regulates contractility, metabolism, autophagy, senescence, and apoptosis in the heart [31]. Circulating IGF-1 levels correlate negatively with the risk of developing cardiovascular diseases [32,33]. On the other hand, cardiac activation of the IGF-1R protects from the detrimental effects of a high-fat diet and myocardial infarction [34,35]. Interestingly, we found that IGF-1R is recruited

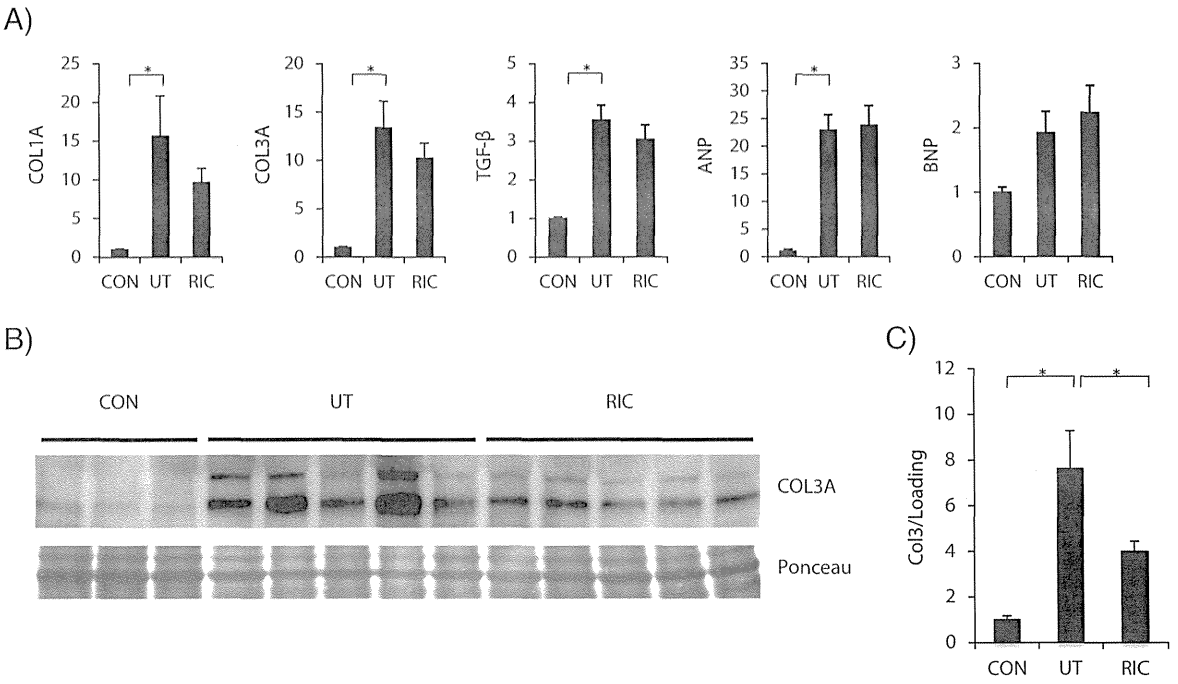

Fig. 4. mRNA expressions and protein level of collagen III. (A) Gene expressions in the marginal infarct region of the untreated and RIC-treated rats, and left ventricle of the CON rats. The bar graph shows the value of each mRNA, corrected for the GAPDH mRNA value. Mean values in the control rat group are represented as 1. The expressions of COL1A, COL3A, and TGF-β in the RIC group tended to be lower than those in the UT group. Values are mean ± SEM. $^*P < 0.05$. (B) Representative Western blot analysis of each group in the marginal area. (C) The value of COL3A protein level at 4 weeks after treatment. Mean values in the CON group are represented as 1. COL3A level was significantly decreased by RIC treatment. Values are mean ± SEM. $^*P < 0.05$. COL1A, collagen type I; COL3A, collagen type III; TGF-β, transforming growth factor-β; ANP, atrial natriuretic peptide; BNP, brain natriuretic peptide.

into the exosomes and is highly expressed in the exosomes by RIC treatment. IGF-1R expression tended to be increased in the skeletal muscles of the RIC group, suggesting that repeated transient ischemic stimulation of the hindlimbs may increase IGF-1R recruitment into the exosomes. Differentiated C2C12 myotube released the IGF-1R contained exosomes, and recruitment of IGF-1R into the exosomes was increased under hypoxic condition. IGF-1R was also highly expressed in the remote non-infarcted myocardium of the RIC group. Therefore, IGF-1R

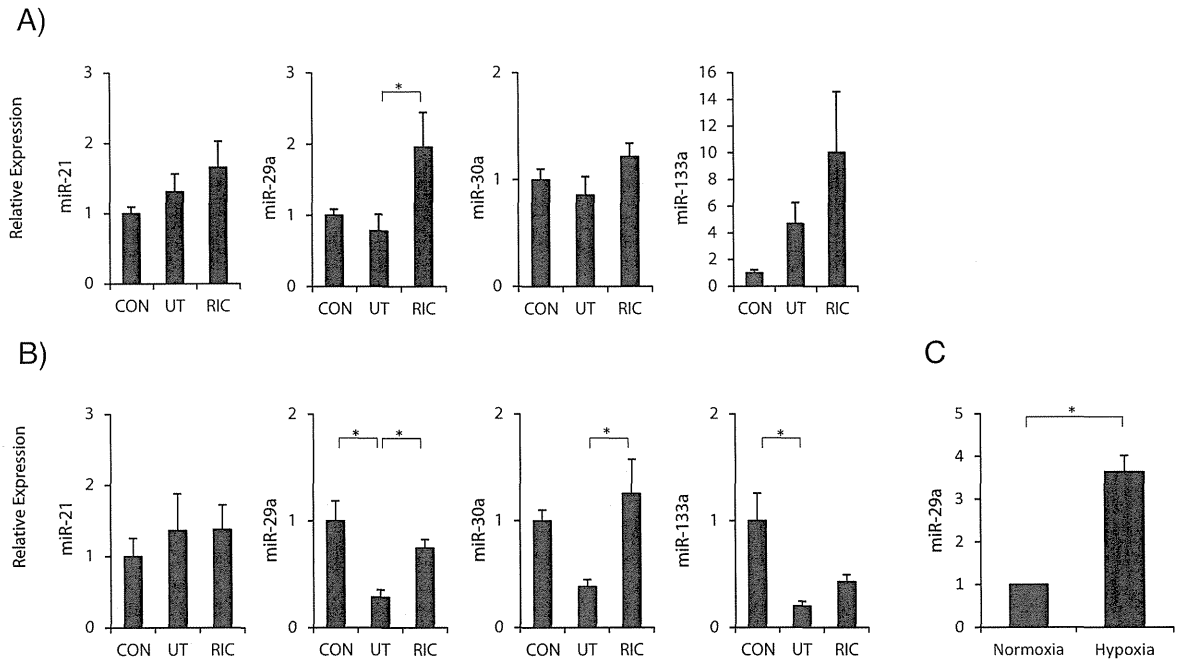

Fig. 5. MicroRNA expressions. (A) RIC treatment increased miR-29a expression in serum exosomes. (B) RIC treatment also increased miR-29a expression in the marginal region of the left ventricle. (C) Hypoxia significantly increased miR-29a expression in exosomes from the media of C2C12 cells. Mean values in the CON group are represented as 1. Values are mean ± SEM ($n = 3$). $^*P < 0.05$. Abbreviations are the same as in Fig. 1 legend.

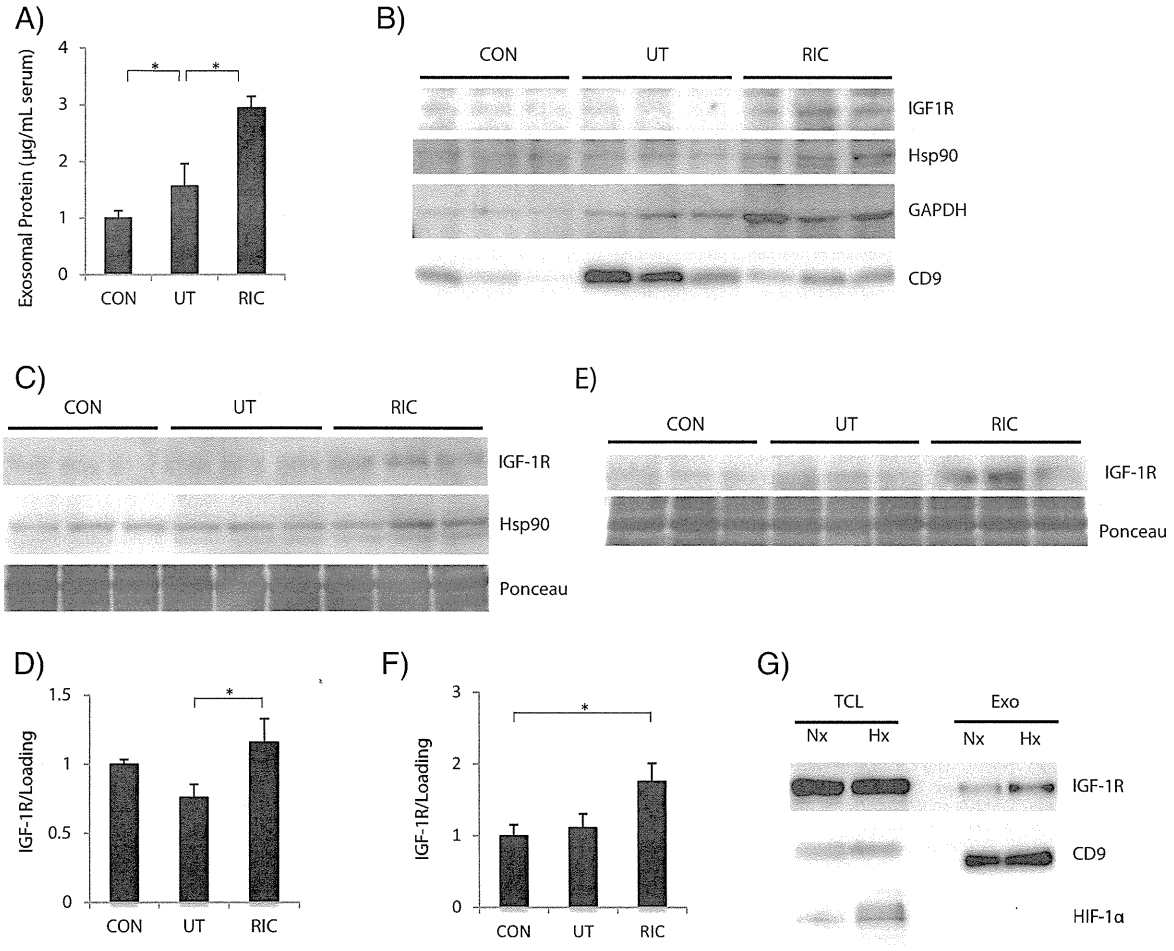

Fig. 6. The protein amount of the serum exosomes and protein levels. (A) RIC treatment significantly increased the protein amount of exosomes. (B) High IGF-1R levels in the serum exosomes were detected in the RIC group. (C) and (D) RIC treatment significantly increased IGF-1R level in the remote non-infarcted myocardium. (E) and (F) IGF-1R level was also increased in skeletal muscles of the hindlimbs of the RIC group. Mean values in the CON group are represented as 1. Values are mean ± SEM (n = each 3). $^*P < 0.05$. (G) Hypoxia increased IGF-1R level in not total cell lysates (TCL) but exosomes (Exo) from culture media. The experiments were repeated three times and similar results were obtained. IGF-1R, insulin-like growth factor 1 receptor. Other abbreviations are the same as in Fig. 1 legend.

may be transported into non-infarcted myocardium from hindlimbs through serum exosomes.

4.1. Study limitation

Any invasive hemodynamic or telemetric analysis was not performed in this study. It is unknown whether hemodynamic status will alter during RIC treatment. The increase of exosomes may be derived from RIC-treated hindlimbs, but the accurate origin is still unidentified. Further studies are needed to elucidate what mechanisms involve the exosomal release by RIC treatment.

In summary, we first demonstrated that RIC treatment attenuates the progressive cardiac dysfunction and remodeling due to an old MI through exosome-mediated intercellular communication. Cardioprotection of RIC treatment may result from the miR-29 family and IGF-1R transportation from the exosome into the heart. Based on these results, RIC treatment is a potentially useful therapeutic approach for CHF.

Funding sources

This study was supported in part by Grant-in-Aid for Scientific Research (24591101, 26460344 and 26461081) from the Ministry of Education, Culture, Sports, Science, and Technology, and Hoansha Foundation.

Conflicts of interest

The authors have no conflicts to report.

Acknowledgments

The authors would like to thank Ms. Chiori Asahi for her technical assistance.

References

[1] C.N. Gring, G.S. Francis, A hard look at angiotensin receptor blockers in heart failure, J. Am. Coll. Cardiol. 44 (2004) 1841–1846.
[2] T.K. Ma, K.K. Kam, B.P. Yan, Y.Y. Lam, Renin–angiotensin–aldosterone system blockade for cardiovascular diseases: current status, Br. J. Pharmacol. 160 (2010) 1273–1292.
[3] M. Packer, M.B. Fowler, E.B. Roecker, et al., Effect of carvedilol on the morbidity of patients with severe chronic heart failure: results of the carvedilol prospective randomized cumulative survival (COPERNICUS) study, Circulation 106 (2002) 2194–2199.
[4] F. Zannad, J.J. McMurray, H. Krum, et al., Eplerenone in patients with systolic heart failure and mild symptoms, N. Engl. J. Med. 364 (2011) 11–21.

[5] R.S. McKelvie, K.K. Teo, N. McCartney, D. Humen, T. Montague, S. Yusuf, Effects of exercise training in patients with congestive heart failure: a critical review, J. Am. Coll. Cardiol. 25 (1995) 789–796.
[6] B.K. Sharma, J.P. Bakker, D.G. McSharry, A.S. Desai, S. Javaheri, A. Malhotra, Adaptive servoventilation for treatment of sleep-disordered breathing in heart failure: a systematic review and meta-analysis, Chest 142 (2012) 1211–1221.
[7] K. Przyklenk, B. Bauer, M. Ovize, R.A. Kloner, P. Whittaker, Regional ischemic preconditioning protects remote virgin myocardium from subsequent sustained coronary occlusion, Circulation 87 (1993) 893–899.
[8] N. Tapuria, Y. Kumar, M.M. Habib, M. Abu Amara, A.M. Seifalian, B.R. Davidson, Remote ischemic preconditioning: a novel protective method from ischemia reperfusion injury—a review, J. Surg. Res. 150 (2008) 304–330.
[9] M. Tanaka, H. Fujiwara, K. Yamasaki, et al., Expression of heat shock protein after ischemic preconditioning in rabbit hearts, Jpn. Circ. J. 62 (1998) 512–516.
[10] F. Kerendi, H. Kin, M.E. Halkos, et al., Remote postconditioning — brief renal ischemia and reperfusion applied before coronary artery reperfusion reduces myocardial infarct size via endogenous activation of adenosine receptors, Basic Res. Cardiol. 100 (2005) 404–412.
[11] M. Wei, P. Xin, S. Li, et al., Repeated remote ischemic postconditioning protects against adverse left ventricular remodeling and improves survival in a rat model of myocardial infarction, Circ. Res. 108 (2011) 1220–1225.
[12] T. Yamazaki, Y. Izumi, Nakamura, et al., Novel device that produces carbon dioxide mist for myocardial infarction treatment in rats, Circ. J. 76 (2012) 1203–1212.
[13] T. Yamazaki, Y. Izumi, Y. Nakamura, et al., Tolvaptan improves left ventricular dysfunction after myocardial infarction in rats, Circ.Heart Fail. 5 (2012) 794–802.
[14] Y. Izumiya, S. Kim, Y. Izumi, et al., Apoptosis signal-regulating kinase 1 plays a pivotal role in angiotensin II-induced cardiac hypertrophy and remodeling, Circ. Res. 93 (2003) 874–883.
[15] T. Yamazaki, N. Yamashita, Y. Izumi, et al., The antifibrotic agent pirfenidone inhibits angiotensin II-induced cardiac hypertrophy in mice, Hypertens. Res. 35 (2012) 34–40.
[16] S. Sano, Y. Izumi, T. Yamaguchi, et al., Lipid synthesis is promoted by hypoxic adipocyte-derived exosomes in 3 T3-L1 cells, Biochem. Biophys. Res. Commun. 445 (2014) 327–333.
[17] A. Harada, S. Okada, D. Konno, et al., Chd2 interacts with H3.3 to determine myogenic cell fate, EMBO J. 31 (2012) 2994–3007.
[18] S. Kurokawa, S. Niwano, H. Niwano, et al., Progression of ventricular remodeling and arrhythmia in the primary hyperoxidative state of glutathione-depleted rats, Circ. J. 75 (2011) 1386–1393.
[19] H. Zhu, G.C. Fan, Role of microRNAs in the reperfused myocardium towards post-infarct remodelling, Cardiovasc. Res. 94 (2012) 284–292.
[20] E. van Rooij, L.B. Sutherland, J.E. Thatcher, et al., Dysregulation of microRNAs after myocardial infarction reveals a role of miR-29 in cardiac fibrosis, Proc. Natl. Acad. Sci. U. S. A. 105 (2008) 13027–13032.
[21] R.F. Duisters, A.J. Tijsen, B. Schroen, et al., miR-133 and miR-30 regulate connective tissue growth factor: implications for a role of microRNAs in myocardial matrix remodeling, Circ. Res. 104 (2009) 170–178.
[22] T. Thum, C. Gross, J. Fiedler, et al., MicroRNA-21 contributes to myocardial disease by stimulating MAP kinase signalling in fibroblasts, Nature 456 (2008) 980–984.
[23] H.E. Botker, R. Kharbanda, M.R. Schmidt, et al., Remote ischaemic conditioning before hospital admission, as a complement to angioplasty, and effect on myocardial salvage in patients with acute myocardial infarction: a randomised trial, Lancet 375 (2010) 727–734.
[24] B.T. Pan, K. Teng, C. Wu, M. Adam, R.M. Johnstone, Electron microscopic evidence for externalization of the transferrin receptor in vesicular form in sheep reticulocytes, J. Cell Biol. 101 (1985) 942–948.
[25] J.S. Schorey, S. Bhatnagar, Exosome function: from tumor immunology to pathogen biology, Traffic 9 (2008) 871–881.
[26] S. Mathivanan, H. Ji, R.J. Simpson, Exosomes: extracellular organelles important in intercellular communication, J. Proteomics 73 (2010) 1907–1920.
[27] E.E. Creemers, A.J. Tijsen, Y.M. Pinto, Circulating microRNAs: novel biomarkers and extracellular communicators in cardiovascular disease? Circ. Res. 110 (2012) 483–495.
[28] S. Matsumoto, Y. Sakata, S. Suna, et al., Circulating p53-responsive microRNAs are predictive indicators of heart failure after acute myocardial infarction, Circ. Res. 113 (2013) 322–326.
[29] P.S. Mitchell, R.K. Parkin, E.M. Kroh, et al., Circulating microRNAs as stable blood-based markers for cancer detection, Proc. Natl. Acad. Sci. U. S. A. 105 (2008) 10513–10518.
[30] J. Skog, T. Wurdinger, S. van Rijn, et al., Glioblastoma microvesicles transport RNA and proteins that promote tumour growth and provide diagnostic biomarkers, Nat. Cell Biol. 10 (2008) 1470–1476.
[31] R. Troncoso, C. Ibarra, J.M. Vicencio, E. Jaimovich, S. Lavandero, New insights into IGF-1 signaling in the heart, Trends Endocrinol. Metab. 25 (2014) 128–137.
[32] P. Spallarossa, C. Brunelli, F. Minuto, et al., Insulin-like growth factor-I and angiographically documented coronary artery disease, Am. J. Cardiol. 77 (1996) 200–202.
[33] Z. Ungvari, A. Csiszar, The emerging role of IGF-1 deficiency in cardiovascular aging: recent advances, J. Gerontol. A Biol. Sci. Med. Sci. 67 (2012) 599–610.
[34] C. Enoki, H. Otani, D. Sato, T. Okada, R. Hattori, H. Imamura, Enhanced mesenchymal cell engraftment by IGF-1 improves left ventricular function in rats undergoing myocardial infarction, Int. J. Cardiol. 138 (2010) 9–18.
[35] K. Huynh, J.R. McMullen, T.L. Julius, et al., Cardiac-specific IGF-1 receptor transgenic expression protects against cardiac fibrosis and diastolic dysfunction in a mouse model of diabetic cardiomyopathy, Diabetes 59 (2010) 1512–1520.

Original Article

Percutaneous Carbon Dioxide Treatment using a Gas Mist Generator Enhances the Collateral Blood Flow in the Ischemic Hindlimb

Yasukatsu Izumi[1, 2], Takehiro Yamaguchi[2], Takanori Yamazaki[2], Naoto Yamashita[1], Yasuhiro Nakamura[2, 3], Masayuki Shiota[1], Masako Tanaka[1, 4], Soichi Sano[2], Mayuko Osada-Oka[1, 5], Kenei Shimada[2], Hideki Wanibuchi[6], Katsuyuki Miura[4], Minoru Yoshiyama[2] and Hiroshi Iwao[1]

Yasukatsu Izumi and Takehiro Yamaguchi contributed equally to this work.

[1]Department of Pharmacology, Osaka City University Medical School, Osaka, Japan
[2]Department of Cardiovascular Medicine, Osaka City University Medical School, Osaka, Japan
[3]Department of Cardiology, Izumi Municipal Hospital, Izumi, Japan
[4]Applied Pharmacology and Therapeutics, Osaka City University Medical School, Osaka, Japan
[5]Food Hygiene and Environmental Health Division of Applied Life Science, Kyoto Prefectural University, Kyoto, Japan
[6]Department of Pathology, Osaka City University Medical School, Osaka, Japan

Aim: Highly concentrated carbon dioxide (CO_2) is thought to be useful for ischemic diseases. We investigated whether treatment with a few micrometers of CO_2 molecules atomized via two fluid-nozzles (CO_2 mist) exerts an angiogenic effect in a mouse ischemic hindlimb model.
Methods: Mice with unilateral hindlimb ischemia were divided into untreated (UT), 100% CO_2 gas alone-treated (CG), mixed air (O_2; 20%, N_2; 80%) mist-treated (AM) and 100% CO_2 mist-treated (CM) groups. The lower body of the mice was encased in a polyethylene bag filled with each gaseous agent using a gas mist generator for 10 minutes daily.
Results: According to a laser Doppler analysis, the ischemic hindlimb blood flow was persistently higher after the seventh day of induction of ischemia in the CM group than in the UT group. The capillary density was also greater in the CM group on day 28 compared with that observed in the UT group. In addition, the parameters in the AM and CG groups were similar to those obtained in the UT group. The observed effects were abolished by the administration of an inhibitor of nitric oxide synthase (NOS). The vascular endothelial growth factor mRNA expression and protein levels and the phosphorylated endothelial NOS level were increased in the CM group compared with that observed in the UT group. A proteomic analysis using liquid chromatography-tandem mass spectrometry identified novel protein candidates regulated by CO_2 mist.
Conclusion: Percutaneous CO_2 mist therapy may be useful for treating ischemia-induced angiogenesis.

J Atheroscler Thromb, 2015; 22:38-51.

Key words: Angiogenesis, Carbon dioxide mist, Ischemia, Peripheral arterial disease, Mass spectrometry

Introduction

Patients with peripheral arterial disease (PAD) exhibit greater functional impairment, with a more rapid functional decline and lower physical activity levels in daily life than those without PAD[1, 2]. The treatment of PAD has evolved over the past decade to include a broad approach, focusing on reducing the incidence of adverse cardiovascular events, improving the symptoms of claudication and preventing tissue loss under conditions of critical limb ischemia[3, 4]. Because these subjects have a severely limited quality of life, great emphasis is placed on ameliorating symptoms and reducing the risk of PAD progression. In

Address for correspondence: Yasukatsu Izumi, Department of Pharmacology, Osaka City University Medical School, 1-4-3 Asahi-machi, Abeno-ku, Osaka 545-8585, Japan
E-mail: izumi@msic.med.osaka-cu.ac.jp
Received: February 4, 2014
Accepted for publication: June 28, 2014

spite of the development of various types of medicines[4], the frequency of PAD has not yet decreased. Exercise rehabilitation is also recommended in patients with this disease[5]; however, supervised exercise is not covered by major medical insurance providers. Furthermore, it can be difficult to provide supervised exercise therapy for patients with PAD who are incapable of performing active exercise, such as those with neurodegenerative and rheumatologic diseases or age-related skeletal muscle wasting. Novel passive exercises, such as thermal therapy and whole-body periodic acceleration therapy, for PAD have been recently received much attention[6, 7].

Balneotherapy using hot springs containing a high concentration of carbon dioxide (CO_2) has long been applied clinically to treat a variety of cardiovascular diseases, especially in European countries. The transfer of CO_2 across the skin is thought to have beneficial local vasomotor effects without inducing systemic hemodynamic modifications[8]. A recent study demonstrated that the immersion of ischemic mouse hindlimbs into baths of artificially created CO_2-enriched water results in a nitric oxide (NO)-dependent increase in collateral blood perfusion as well as the induction of regional vascular endothelial growth factor (VEGF) synthesis[9]. Hence, bathing in CO_2-enriched water may be a useful therapeutic approach in patients with PAD. Carbonate spring water is generally defined as water containing more than 1,000 parts per million (ppm) of CO_2, although the cost to set up such systems is expensive. Therefore, the development of more simple and affordable systems would be valuable.

Very recently, a new and simple system was developed in which CO_2 gas is dissolved in water containing a high concentration of CO_2 molecules using two fluid-nozzles, namely, CO_2 mist. We previously reported that the CO_2 mist produced by this device has a therapeutic benefit in the treatment of heart failure due to myocardial infarction[10].

In the present study, we investigated whether treatment with CO_2 mist accelerates angiogenesis in a well-established mouse model of ischemia-induced angiogenesis. Consequently, we obtained evidence that CO_2 mist therapy stimulates ischemia-induced revascularization via upregulation of the angiogenic growth factor expression.

Materials and Methods

Animals and Experimental Protocol

All procedures involving animals were performed in compliance with the Osaka City University animal care guidelines. The study protocol conformed with the Guidelines for the Care and Use of Laboratory Animals published by the US National Institutes of Health (NIH publication No. 85-23, revised 1996). Male Wistar rats and male C57BL/6J (wild-type), inducible NO synthase deficient ($iNOS^{-/-}$) and endothelial NO synthase deficient ($eNOS^{-/-}$) mice 8-10 weeks of age were used in the present study. Unilateral hindlimb ischemia was induced under anesthesia with sodium pentobarbital (50 mg/kg intraperitoneally (i.p.)), as previously described[7, 11-12]. Mixed air dry mist (AM) and CO_2 mist (CM) was generated using a dry mist production unit (Advance Biotron Co., Ltd., Tokyo, Japan)[10]. In brief, 100% concentrated CO_2 or mixed air (N_2: 80%; O_2: 20%) was compounded and compressed with water through double fluid nozzles at 4 atmospheres.

The mice were treated with 100% CO_2 gas (CG), AM or CM for 10 minutes once a day in a draft cabinet. Briefly, under anesthesia with sodium pentobarbital, the lower body of each mouse was encased in a sealed polyethylene bag on a heating plate at 37℃. The polyethylene bag was then filled with CG, AM or CM in the draft cabinet. The untreated (UT) group was kept on the heating plate at 37℃ for 10 minutes once a day under anesthesia. The use of 100% CO_2 at 4 units of barometric pressure resulted in a CO_2 concentration in the bag of approximately 900,000 ppm[10].

Effects of CO_2 Mist on the Vasodilation of Microvessels and Tissue Blood Flow

The first series of experiments was performed to compare the effects of CG, AM and CM on the vasodilation of microvessels. One week after the induction of hindlimb ischemia, the mouse femurs were slightly cut open, exposing the subcutaneous vessels, under anesthesia with sodium pentobarbital (50 mg/kg, i.p.). The incision site was then covered with a transparent seal. We then observed whether the CG or CM treatment dilated the microvessels using a digital microscope (VHX-1000, Keyence Co., Ltd., Osaka, Japan) equipped with a zoom lens.

Next, we investigated the effects of CG and CM on the tissue blood flow. At one week after the induction of hindlimb ischemia in the rats, we measured the blood flow in the shallow region of the tissue using laser tissue blood oxygenation monitors and near-infrared spectroscopy (BOM-L1TR SF, Omegawave Inc., Tokyo, Japan) during treatment with CG or CM. In brief, a saturation-monitoring sensor was attached to the rat toe. Changes in the tissue levels of oxygenated hemoglobin (oxy-Hb), deoxygenated hemoglobin

(deoxy-Hb), total hemoglobin (total-Hb) and tissue saturation (StO_2) compared with that observed at baseline were measured continuously during and after the 10-minute treatment period[10].

Laser Doppler Blood Flow Analysis

In order to investigate the effects of a long duration of CG, AM or CM treatment on the hindlimb blood flow, mice with induced ischemia were randomly divided into four groups: the UT, CG, AM and CM groups. We performed the same experiment twice and obtained data for a total of a 42 mice. The hindlimb blood flow was assessed under anesthesia with sodium pentobarbital (50 mg/kg, i.p.) using a laser Doppler blood flow (LDBF) analyzer (Moor LDI; Moor Instruments, Devon, UK) before and immediately after surgery and on postoperative days 4, 7, 14, 21 and 28, as previously described[11, 12]. The LDBF analysis was performed before each treatment session on days 4, 7, 14 and 21 and 24 hours after the last treatment. After the scanning blood flow, the stored images were subjected to computer-assisted quantification, and the average flow in the ischemic and non-ischemic limbs was calculated. In order to prevent data variations resulting from the effects of ambient light and temperature, the hindlimb blood flow was expressed as the ratio of the left (ischemic) to the right (non-ischemic) LDBF values.

Capillary Density

At 28 days after surgery, the mice were euthanized under anesthesia with sodium pentobarbital (100 mg/kg, i.p.), and their hindlimbs were removed. The capillary density within the ischemic thigh adductor skeletal muscles was subsequently analyzed in order to obtain specific evidence of vascularity at the level of the microcirculation. Three sections of ischemic muscle were harvested from each animal, sliced and fixed in methanol. The tissues were then embedded in paraffin, and multiple tissue slices of 5 μm in thickness were prepared. Capillary endothelial cells (ECs) were identified using immunohistochemical staining with a rat anti-mouse CD31 antibody (Ab) (Pharmingen, CA). Fifteen random microscopic fields from three different sections in each tissue block were examined for the presence of capillary ECs, and the capillary density was expressed as the number of capillaries per high-power field ($\times 400$)[11, 12].

Measurement of the Nitrate (NO_3^-) Levels in the Serum

At 28 days after surgery, the mouse serum nitrate (NO_3^-) concentration was measured using high-performance liquid chromatography, according to the manufacturer's instructions[10].

Quantitative Real-Time Polymerase Chain Reaction

Total RNA was isolated using ISOGEN (Nippon Gene Co., Ltd., Toyama, Japan). In order to determine the transcript levels of vascular endothelial growth factor (VEGF) and fibroblast growth factor 2 (FGF-2), the RNA samples were subjected to quantitative real-time polymerase chain reaction (RT-PCR, 7500 Fast; Applied Biosystems, Carlsbad, CA). One-step quantitative RT-PCR reactions were performed using 100 ng of total RNA per reaction. The transcript levels were normalized to that of 18S for the analysis.

Effects of a NO Synthase Inhibitor on the Outcomes of CO_2 Dry Mist Therapy

In order to chronically inhibit NOS, wild-type mice with hindlimb ischemia were provided water containing 1 mg/mL of N^G-nitro- L-arginine methyl ester (L-NAME) for four weeks. Furthermore, $iNOS^{-/-}$ and $eNOS^{-/-}$ mice with hindlimb ischemia were treated with CO_2 mist for 28 days. The hindlimb blood flow was then measured, as described above.

Effects of a Low Concentration of CO_2 on the Tissue Blood Flow

In order to investigate whether blood perfusion is enhanced in a CO_2 concentration-dependent manner, we compared the effects of no treatment and treatment with 250,000 ppm (low CM) or 900,000 ppm (high CM) of CO_2 in the bags encasing the lower body of the mice. The high or low CM conditions were produced using 100% concentrated CO_2 or a mixture of 100% concentrated CO_2 and mixed air, respectively. The LDBF analysis was performed as described above.

Mass Analysis

At four days after ischemia, the mice were euthanized under anesthesia with sodium pentobarbital (100 mg/kg, i.p.) and their hindlimbs were removed. Digested proteins (150 μg) from the muscles in the non-ischemic, UT and CM groups (pooling of each $n=5$) were reduced, alkylated, digested with trypsin and labeled with an isobaric tag for use with relative and absolute quantitation (iTRAQ) reagents (AB Sciex, Framingham, MA), according to the manufacturer's instructions, with the following minor modification.

After the labeling reaction (114, non-ischemic; 116, UT; 117, CM), the three samples were pooled

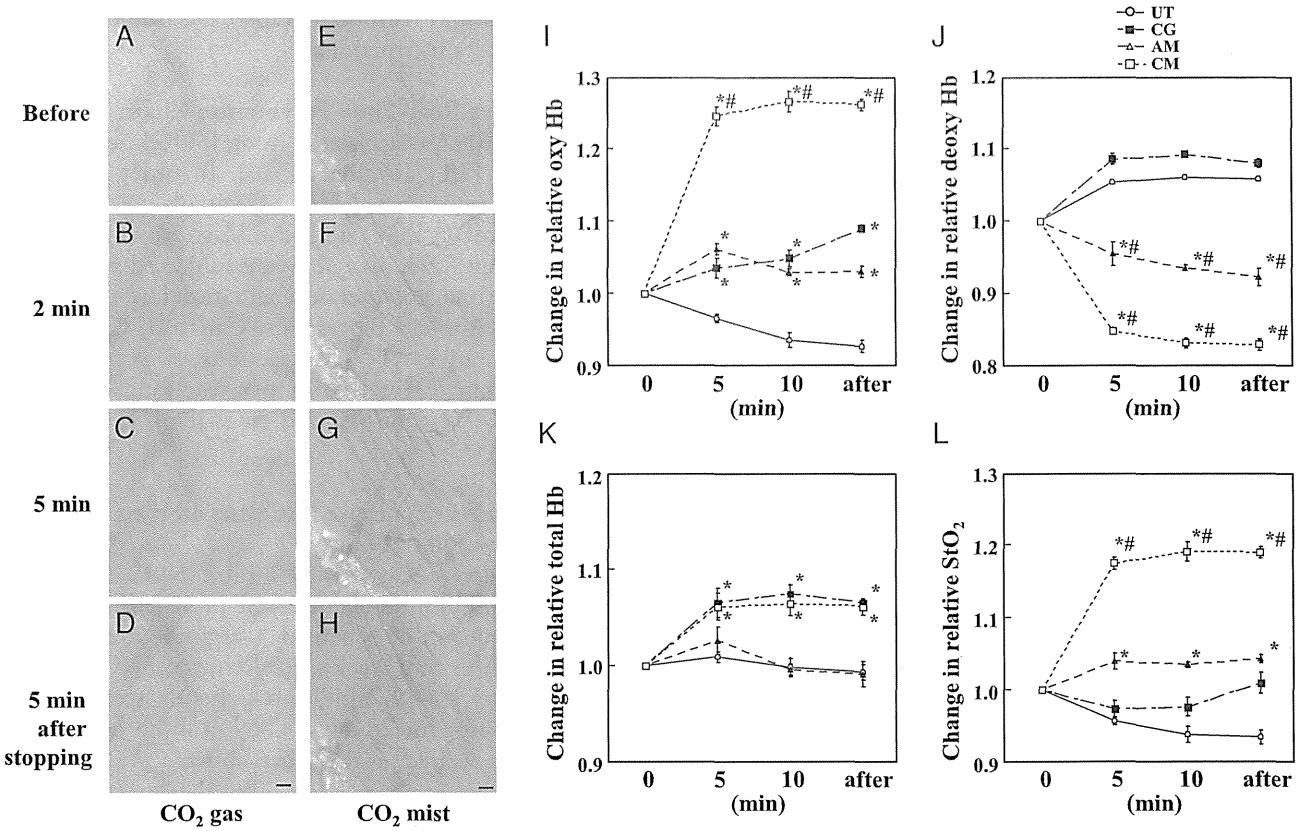

Fig. 1. Vasodilatory effects of the CO_2 mist and changes in the relative tissue blood flow. Photographs (A to H) taken with a digital microscope showing the vasodilatory effects of the CO_2 gas (A to D) and CO_2 mist (E to H) in the femoral subcutaneous tissue. After two minutes of spraying the CO_2 mist, microvessels gradually appeared. These microvessels were more prominent after five minutes of spraying the CO_2 mist (G) compared with that observed before treatment (E). Bar = 100 μm. The CO_2 mist group had significantly increased oxygenated hemoglobin (Hb) levels (I) and decreased deoxygenated Hb levels (J) compared with the untreated, air mist and CO_2 gas groups. The total Hb levels were increased versus baseline in the CO_2 gas and CO_2 mist groups, but not the untreated and air mist groups (K). The tissue saturation levels were also significantly increased in the CO_2 mist (CM) group compared with those observed in the untreated (UT), air mist (AM) and CO_2 gas (CG) groups (L). oxy Hb, oxygenated hemoglobin; deoxy Hb, deoxygenated hemoglobin; total Hb, total hemoglobin; StO_2, tissue saturation. Each bar represents the mean ± SEM. $^*p<0.05$ vs. UT; $^\#p<0.05$, CO_2 mist vs. CO_2 gas.

and 10 μL of 20% (v/v) trifluoroacetic acid was added to cleave RapiGest (Waters, Milford, MA). The samples were then vortexed, incubated at 37℃ for one hour and centrifuged. The supernatant was subsequently purified using a cation exchange column (AB Sciex), according to standard procedures.

Next, a proteome analysis was performed using a DiNa-AI nano LC System (KYA Technologies, Tokyo, Japan) coupled with a QSTAR Elite hybrid mass spectrometer (AB Sciex) through a NanoSpray ion source (AB Sciex), as previously described[13]. Briefly, mobile phase A included 98% water (2% acetonitrile [ACN], 0.1% formic acid) and mobile phase B included 70% ACN (0.1% formic acid, 30% water). The column effluent was introduced into the spray chamber through a tapered stainless steel emitter and directly electrosprayed into the QSTAR System ion trap mass spectrometer in the positive mode for the nanoESI-tandem mass spectrometry (MS/MS) analysis. One sample was run for 150 minutes. Protein identification was performed using the Analyst QS Software 2.0 program (AB Sciex) in the positive-ion mode. Both sets of data were processed using the ProteinPilot Software 2.0.1 package according to the ParagonTM search algorithm (AB Sciex), and the MS/MS data were searched against the NCBI database using a *Mus musculus* taxonomy filter. The minimum threshold for protein identification was set at a protein score of 1.3,

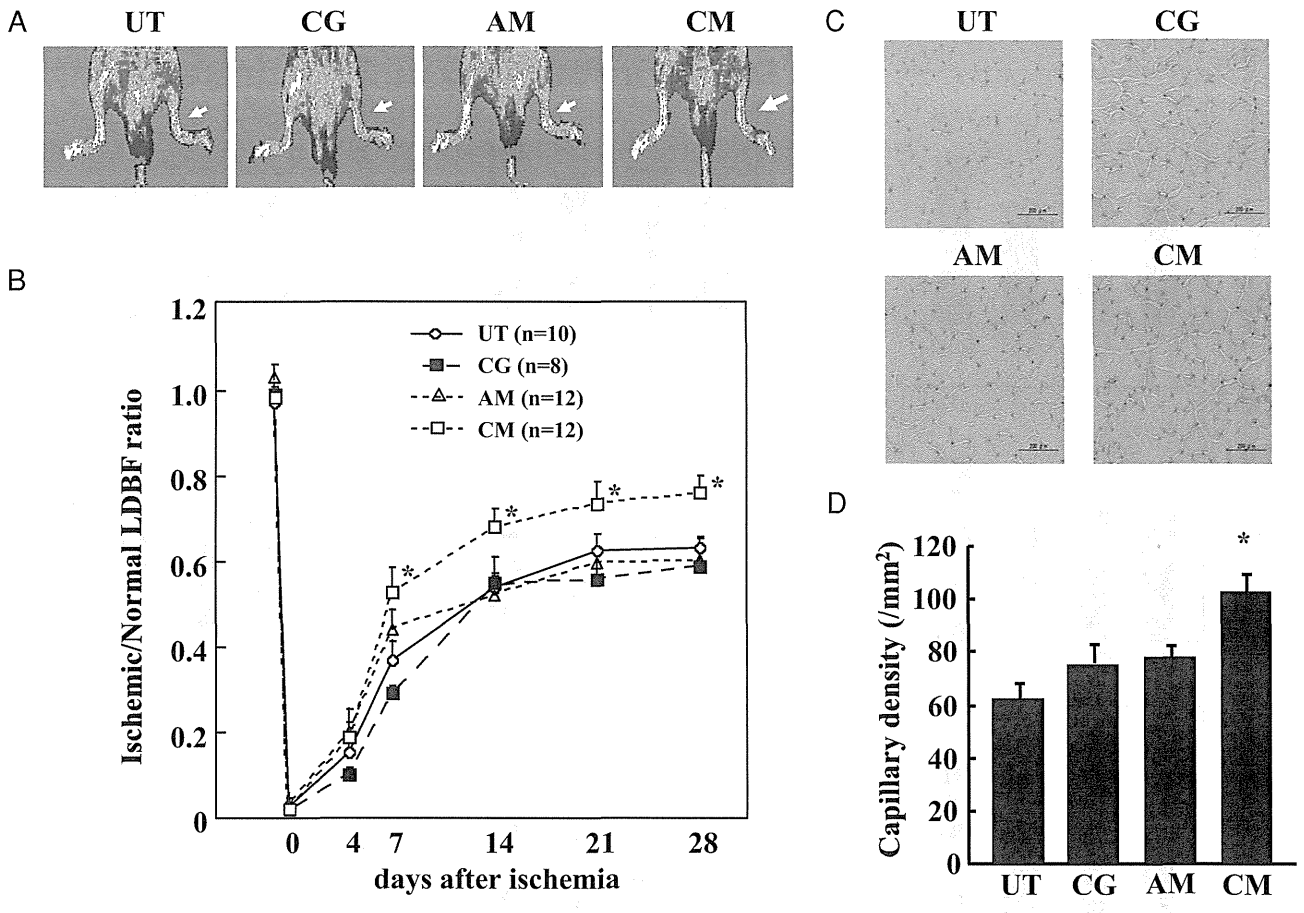

Fig. 2. Laser Doppler blood flow (LDBF) analysis and capillary density. (A) A representative LDBF image. A low-perfusion signal was observed in the ischemic hindlimbs of the untreated mice, whereas a high-perfusion pattern (white to red) was detected in the CO_2 mist-treated mice. The abbreviations are the same as in the Fig. 1 legend. (B) The computer-assisted quantitative analysis of hindlimb blood perfusion showed a significant improvement in the ischemic/normal hindlimb blood flow ratio in the CO_2 mist-treated mice compared with that seen in the untreated, CO_2 gas and air mist groups. Each bar represents the mean ± SEM. $^*p<0.05$ vs. UT at each time point. (C) Representative angiograms and (D) capillary density assessed according to staining with anti-CD31 Abs on postoperative day 28. Each bar represents the mean ± SEM. $^*p<0.05$ vs. UT.

which corresponded to a confidence level above 95% and a false discovery rate of 1%.

Western Blotting

Our detailed methods have been previously described[11, 12]. Protein extracts were obtained from homogenized ischemic or non-ischemic skeletal muscles and electrophoretically transferred to polyvinylidene difluoride membranes (Immobilon-P, Millipore, Billerica, MA). The membranes were then probed with each primary antibody.

Antibodies were obtained from the following sources: anti-Ras-associated protein 1b (Rap1b), superoxide dismutase 2 (SOD2), glyceraldehyde-3-phosphate dehydrogenase (GAPDH), VEGF, FGF-2 and actin antibodies from Santa Cruz Biotechnology (Dallas, TX); phosphor-ERK1/2 and anti-phospho-eNOS (p-Ser1177) antibodies from Cell Signaling Technology (Beverly, MA); anti-eNOS antibodies from BD Biosciences (San Jose, CA).

Statistical Analysis

All data are presented as the mean ± standard error of the mean (SEM). Comparisons between two experimental groups were made to test for statistical significance using Student's *t*-test. Further comparisons between groups were made according to the Tukey-Kramer method using the StatView software program (SAS Institute, Inc., Cary, North Carolina, USA). Differences were considered to be statistically

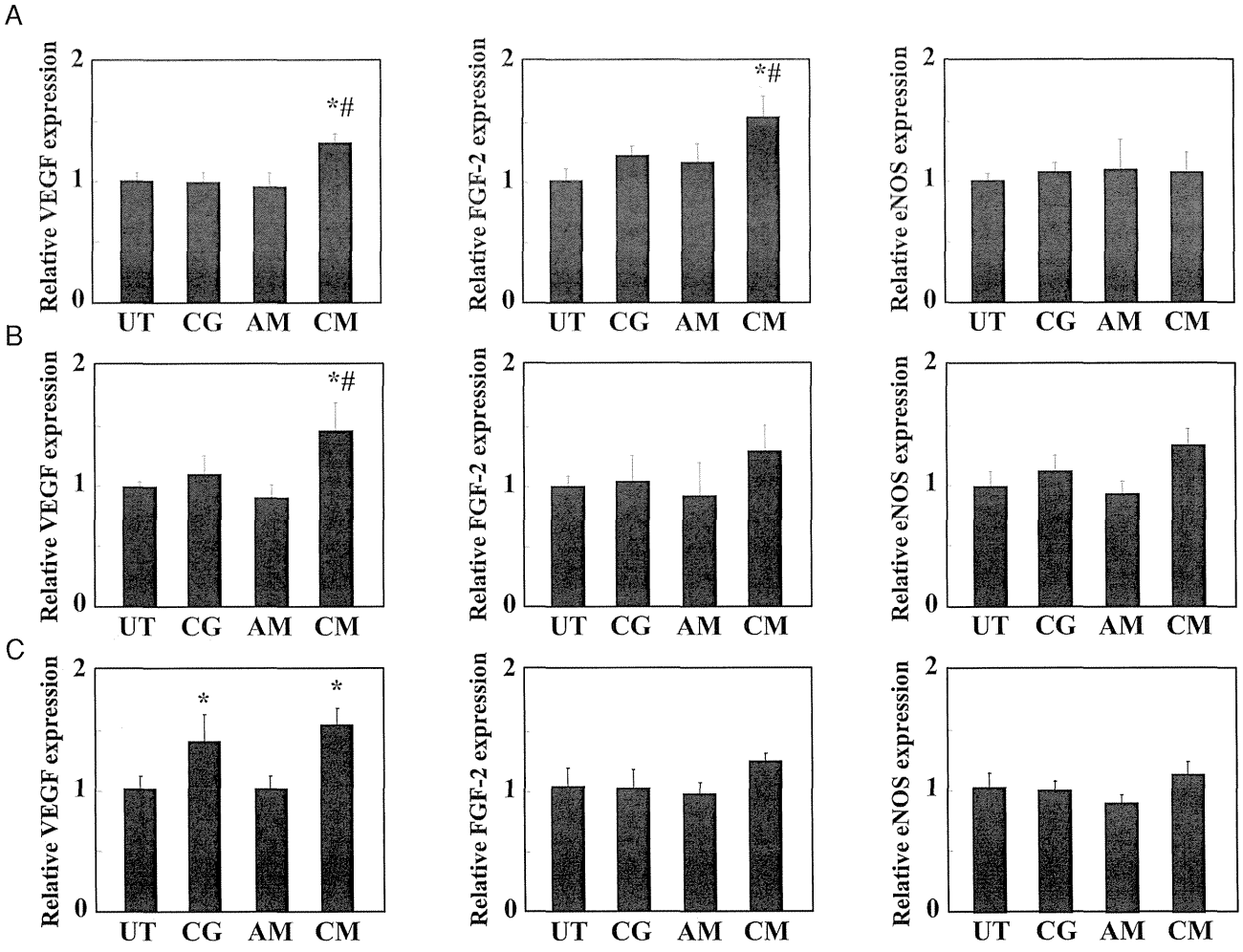

Fig. 3. Gene expression levels in the ischemic hindlimbs of the untreated, CO_2 gas, air mist-treated and CO_2 mist-treated mice. The bar graph shows each mRNA level corrected for the 18S rRNA level on postoperative day 4 (A), day 7 (B) and day 14 (C). The mean value in the untreated group was set at 1. The VEGF and FGF-2 expression levels were significantly increased by the CO_2 mist treatment. VEGF, vascular endothelial growth factor; FGF-2, fibroblast growth factor-2; eNOS, endothelial nitric oxide synthase. Other abbreviations are the same as in the Fig. 1 legend. The values are presented as the mean ± SEM ($n=8$ to 12 (A) and (B), $n=4$ to 6 (C)). $^{*}p<0.05$ vs. UT; $^{\#}p<0.05$, CO_2 mist vs. CO_2 gas.

significant at a value of $p<0.05$.

Results

Effects of CO_2 Mist on Vasodilation and the Tissue Blood Flow

We compared the effects of treatment with CG, AM and CM on vasodilation. Wild-type mice in a transparent acrylic case were treated with CG, AM or CM. Treatment with CG did not change the detection of microvessels compared with that observed before treatment (**Fig. 1-A** to **D**), nor did AM treatment (data not shown). In contrast, a few microvessels were gradually detected two to five minutes after treatment with the CO_2 mist compared with that noted before treatment (**Fig. 1-E** to **H**).

Next, we measured the changes in the relative tissue blood flow during CG, AM and CM treatment (**Fig. 1-I** to **L**). Rats were used in this experiment because the mice were too small to precisely measure the tissue blood flow. The CM group exhibited increased oxy-Hb levels (1.26-fold; **Fig. 1-I**), decreased deoxy-Hb levels (0.83-fold; **Fig. 1-J**) and increased StO_2 levels (1.19-fold; **Fig. 1-L**) compared with that observed at baseline. Importantly, the CM group exhibited significantly higher oxy-Hb levels than the

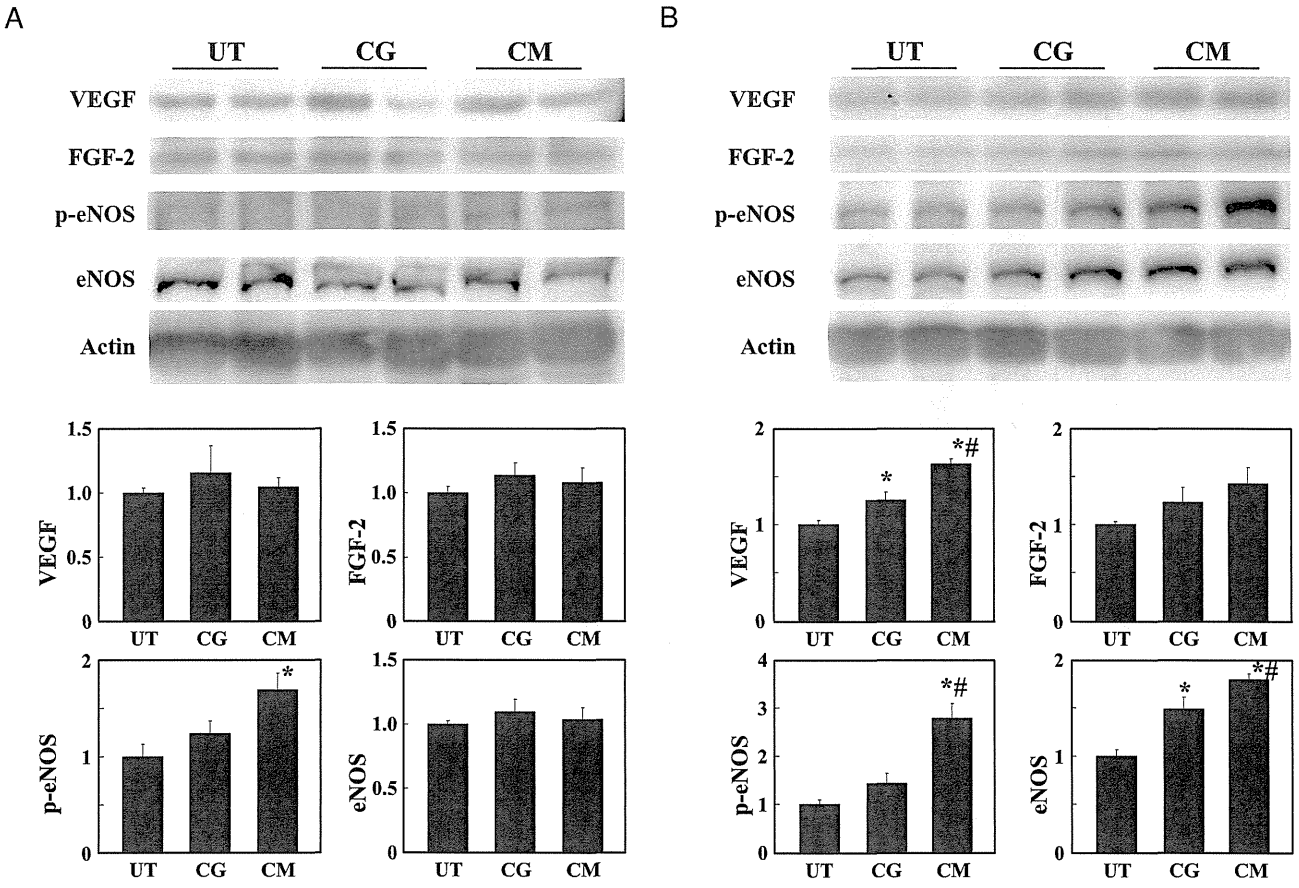

Fig. 4. Protein levels in the ischemic hindlimbs of the untreated and CO_2 gas- and CO_2 mist-treated mice. The upper panels show the findings of a representative Western blot analysis. The lower bar graphs show the level of each protein on postoperative day 4 (A) and day 14 (B) in the ischemic hindlimbs of the untreated and CO_2 gas- and CO_2 mist-treated mice. The mean value in the untreated group was set at 1. The VEGF and phosphorylated eNOS levels were significantly increased by the CO_2 mist treatment on day 14. p-eNOS, phosphorylated eNOS. Other abbreviations are the same as in the Fig. 3 legend. The values are presented as the mean ± SEM ($n=4$ to 6). $^{*}p<0.05$ vs. UT; $^{\#}p<0.05$, CO_2 mist vs. CO_2 gas.

UT group, as well as the CG and AM groups, after five minute of each treatment. Conversely, the CM group exhibited significantly lower deoxy-Hb levels than the UT, AM and CG groups after five minutes of each treatment. Interestingly, the StO_2 levels were also significantly higher in the CM group than in the CG group, although the total-Hb levels in the CM group were similar to those observed in the CG group (**Fig. 1-L**).

Laser Doppler Blood Perfusion and Tissue Capillary Density

We subsequently investigated whether treatment with CM accelerates blood flow recovery after ischemia. Immediately after the left femoral artery and vein were resected, the ratio of the ischemic (left) to non-ischemic (right) hindlimb LDBF (the LDBF ratio) decreased by <0.05 in all groups. However, the CM-treated mice showed a significant blood flow recovery in the ischemic limb compared with the UT mice (day 14: 0.71 ± 0.04 vs 0.54 ± 0.03, day 28: 0.78 ± 0.04 vs 0.63 ± 0.02, $p<0.05$, respectively; **Fig. 2-A** and **B**), whereas the CG- and AM-treated mice demonstrated no acceleration in the recovery of the blood flow.

Next, we measured the capillary density in histological sections harvested from the ischemic tissues in order to investigate the extent of angiogenesis at the level of the microcirculation (**Fig. 2-C**). A quantitative analysis revealed that the capillary density was significantly greater on postoperative day 28 in the CM mice than in the UT mice (**Fig. 2-D**).

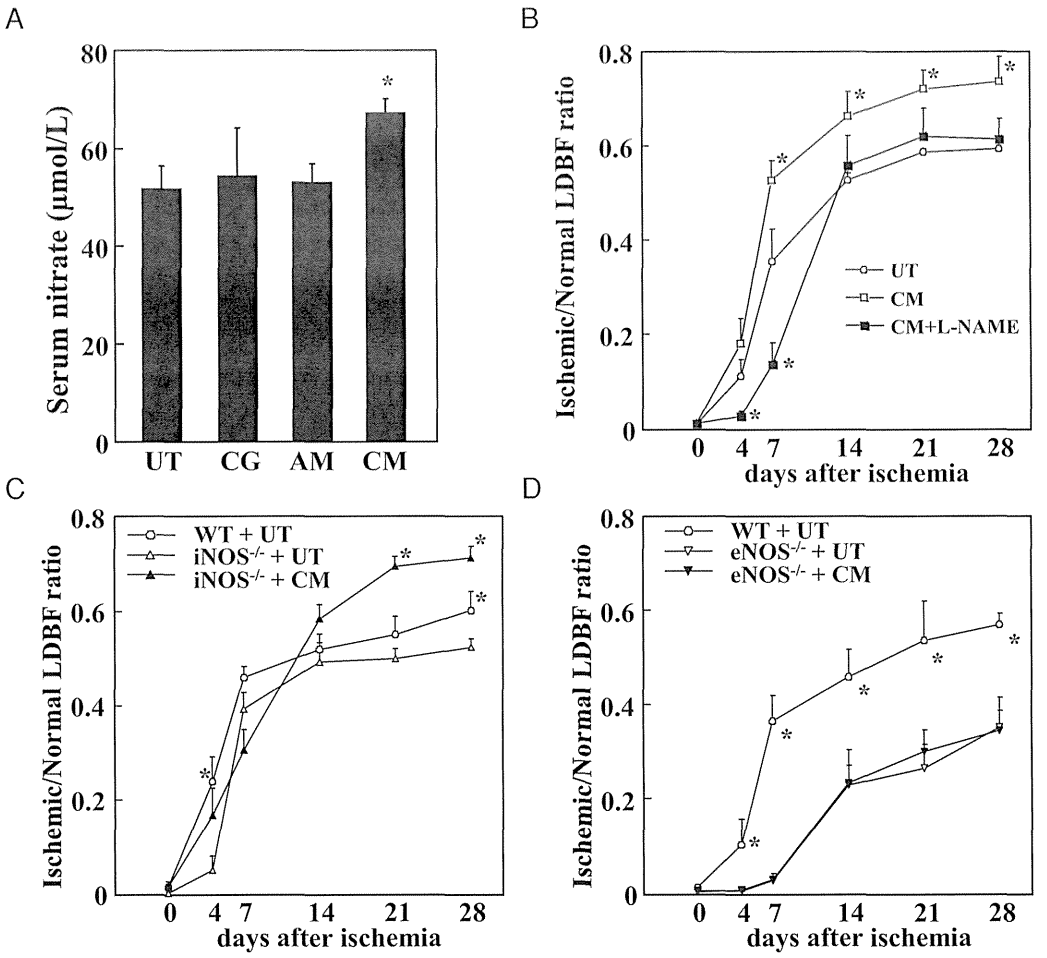

Fig. 5. Serum concentrations of nitrate and results of the LDBF analysis following NOS inhibition. (A) The serum concentrations of nitrate (NO_3^-) were significantly greater in the CM group than in the UT group on postoperative day 4. In contrast, the serum concentrations of NO_3^- in the CG and AM group did not differ significantly from the control values. The values are presented as the mean ± SEM (n=6 to 8). *p<0.05 vs. UT. (B) The administration of l-NAME (1 mg/mL in drinking water) reduced the increase in perfusion induced by the CO_2 mist to a normal level. The values are presented as the mean ± SEM (n=6 to 8). *p<0.05 vs. UT at each time point. (C) Treatment with CO_2 mist accelerated the recovery of the blood flow after ischemia in the iNOS$^{-/-}$ mice. The values are presented as the mean ± SEM (n=6 to 8). *p<0.05 vs. iNOS$^{-/-}$ + UT at each time point. In contrast, the CO_2 mist failed to increase the recovery of the blood flow in the eNOS$^{-/-}$ mice (D). The values are presented as the mean ± SEM (n=6 to 8). *p<0.05 vs. eNOS$^{-/-}$ + UT at each time point.

Expression of Angiogenic Growth Factors in the Ischemic Hindlimbs

VEGF and FGF-2 are the major cytokines responsible for ischemia-induced angiogenesis and arteriogenesis. Therefore, we examined the expression levels of VEGF and FGF-2 in the ischemic tissues of each group. Consequently, a quantitative RT-PCR analysis showed a significantly greater expression of VEGF on days 4, 7 and 14 and FGF2 on day 4 in the CM-treated mice compared with the UT mice (**Fig. 3-A, B** and **C**). On the other hand, the eNOS expression was slightly but not significantly increased by CM treatment, whereas treatment with CG did not change the VEGF expression on days 4 and 7, but rather increased the expression on day 14.

We also examined the protein levels using a Western blot analysis. As shown in **Fig. 4**, the VEGF protein levels were increased in the CM group compared with those observed in the UT group. Meanwhile, the FGF-2 levels tended to be increased in the

CM group (p=0.055 vs. UT). In contrast to the mRNA expression, the level of phosphorylated eNOS was significantly increased in the CM group on both days 4 and 14. There were no differences in the actin levels between the groups.

Effects of CO_2 Mist Treatment on the NO and NOS Levels

The serum concentration of nitrate was measured at four days after ischemia, as shown in **Fig. 5-A**. The serum nitrate concentrations were significantly greater in the CM group than in the UT group ($p<$ 0.05), whereas the nitrate levels in the CG and AM groups did not differ from the control values.

Next, the effects of the NO signaling pathway were investigated. Consequently, L-NAME completely inhibited the effects of the CM treatment (**Fig. 5-B**). Furthermore, the CM treatment significantly increased the LDBF ratio in the iNOS-deficient mice, but not in the eNOS-deficient mice (**Fig. 5-C** and **D**). These results suggest that the actions of CO_2 mist in stimulating revascularization *in vivo* are dependent, at least in part, on eNOS.

Effects of a Low Concentration of CO_2 Mist on the Tissue Blood Flow

We compared the differences in blood flow recovery in the ischemic hindlimbs between treatment with high and low CM concentrations. Similar to previous results, treatment with high CM significantly accelerated the blood flow recovery in the ischemic hindlimbs. On the other hand, treatment with low CM only slightly recovered the blood flow in the ischemic hindlimbs (**Fig. 6**), suggesting that recovery of the blood flow is enhanced in a CO_2 concentration-dependent manner.

Mass Analysis

In order to further investigate the detailed mechanisms of action of CM treatment, we performed a proteomic analysis of the hindlimb muscles at four days after ischemia. Proteins from the adductor muscle in the non-ischemic, UT and CM groups were labeled with 114, 116 and 117 tags, respectively, and 195 proteins were identified when the protein threshold was set at 1.3 to achieve a confidence level above 95%. We also included an additional 1.2-fold change cutoff for the iTRAQ ratio (116/114 <0.80 or >1.2) in order to reduce the rate of false-positive results for classifying proteins as upregulated or downregulated. Among the 195 proteins identified, 68 were upregulated and 62 were downregulated by ischemia. Furthermore, 18 of the 68 upregulated proteins were downregulated by

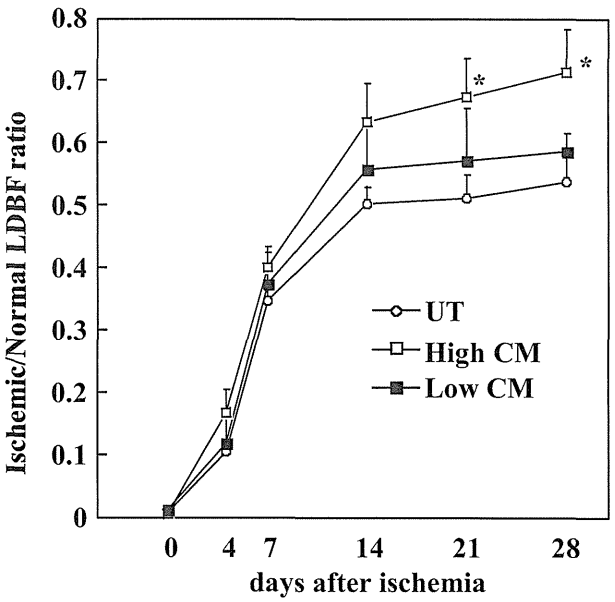

Fig. 6. Effects of high and low concentrations of CO_2 mist on ischemia-induced angiogenesis. Treatment with CO_2 mist at a high concentration of CO_2 (High CM) accelerated the blood flow recovery in the ischemic hindlimbs, whereas treatment with CO_2 mist at a low concentration of CO_2 (Low CM) only slightly recovered the blood flow. Each bar represents the mean ± SEM (n=each 6). *$p<0.05$ vs. UT at each time point.

CM treatment (ratio: 116/117 <0.80). As shown in **Table 1-A**, some of these proteins were related to signal transduction. In contrast, 21 of the 62 downregulated proteins were upregulated by CM treatment (ratio: 116/117 >1.2). As shown in **Table 1-B**, some of these proteins were related to metabolic enzymes.

In order to confirm the results of the mass analysis, we investigated the levels of several proteins using Western blotting (**Supplemental Fig. 1**). Consequently, the Rap1b level was remarkably increased by ischemia and subsequently decreased by CM treatment. In addition, the SOD-2 and GAPDH levels were decreased by ischemia and increased by CM treatment.

Discussion

The major findings of the present study are that angiogenesis and blood flow recovery in response to hindlimb ischemia were significantly improved by CO_2 mist treatment. Furthermore, we obtained the first evidence that CO_2 mist therapy affects both eNOS and VEGF, as well as the glycolytic system. Therefore, CO_2 mist treatment accelerates ischemia-induced

Table 1. Lists of the 18 proteins decreased by CO_2 mist among the 68 proteins upregulated by ischemia (A) and the 21 proteins increased by CO_2 mist among the 62 proteins downregulated by ischemia (B)

A

Accession No.	Name	Ischemia/ non-ischemia	Ischemia + CO_2 mist/Ischemia
gi|51172612	group specific component precursor	3.0807	0.6645
gi|12963497	kininogen 1 isoform 2	3.8908	0.6651
gi|160358829	hemopexin precursor	3.9433	0.7323
gi|6678768	myristoylated alanine rich protein kinase C substrate	6.2190	0.7396
gi|33563236	Rho, GDP dissociation inhibitor (GDI) beta	9.1627	0.7432
gi|149272386	PREDICTED: similar to thymosin beta-4	5.7131	0.7498
gi|33859753	RAS related protein 1b precursor	3.1921	0.7591
gi|124486712	ribosome binding protein 1 isoform a	3.3542	0.7599
gi|145301578	hemoglobin alpha 1 chain	2.7937	0.7624
gi|86476077	thymosin, beta 10	6.7223	0.7717
gi|21313162	RAB1B, member RAS oncogene family	1.9955	0.7815
gi|7110705	prothymosin alpha	4.1927	0.7853
gi|6681079	cathepsin B preproprotein	5.3743	0.7881
gi|6680836	calreticulin precursor	2.8233	0.7890
gi|18252782	serpin peptidase inhibitor, clade C, member 1 precursor	2.7453	0.7934
gi|6671549	peroxiredoxin	1.3707	0.7943
gi|12963729	INO80 complex subunit B	1.3092	0.7948
gi|6679439	peptidylprolyl isomerase A	2.9372	0.7985

B

Accession No.	Name	Ischemia/ non-ischemia	Ischemia + CO_2 mist/Ischemia
gi|130488506	four and a half LIM domains 3	0.6897	1.6215
gi|21313458	nucleolar protein 3	0.5381	1.6085
gi|149253821	PREDICTED: similar to Glyceraldehyde-3-phosphate dehydrogenase (GAPDH) isoform 2	0.4492	1.5665
gi|114431240	adenosine monophosphate deaminase 1 (isoform M)	0.4481	1.5416
gi|33563266	NADH dehydrogenase (ubiquinone) 1 alpha subcomplex, 4	0.4739	1.4803
gi|149266429	PREDICTED: similar to Glyceraldehyde-3-phosphate dehydrogenase isoform 2	0.5879	1.3685
gi|21313679	ATP synthase, H + transporting, mitochondrial F0 complex, subunit d	0.5153	1.3574
gi|257743039	lactate dehydrogenase A isoform 2	0.5176	1.3055
gi|149265502	PREDICTED: similar to Glyceraldehyde-3-phosphate dehydrogenase (GAPDH)	0.6516	1.2813
gi|33859811	mitochondrial trifunctional protein, alpha subunit precursor	0.7632	1.2807
gi|227430322	calsequestrin 1	0.7146	1.2730
gi|20452466	ferrochelatase	0.7089	1.2654
gi|6671762	muscle creatine kinase	0.5491	1.2503
gi|254553458	glucose phosphate isomerase 1	0.6630	1.2444
gi|31980762	superoxide dismutase 2, mitochondrial precursor	0.6287	1.2396
gi|40254393	hypothetical protein LOC66273	0.6046	1.2388
gi|6755256	muscle glycogen phosphorylase	0.5423	1.2289
gi|6671539	fructose-bisphosphate aldolase A	0.5888	1.2247
gi|6679651	enolase 3, beta muscle isoform 1	0.5824	1.2119
gi|6671519	adenylosuccinate synthase like 1	0.6999	1.2027
gi|6678391	troponin I, skeletal, fast 2	0.6375	1.2019